

INVESTIGATION OF THE MICROSTRUCTURAL AND MECHANICAL PROPERTIES OF
SELECTIVELY LASER MELTED IN718 OVERHANGS FABRICATED WITHOUT
SUPPORT STRUCTURES

by

MANJUNATH HANUMANATHA

Presented to the Faculty of the Graduate School of

The University of Texas at Arlington

in partial fulfillment of the requirements

for the degree of

MASTER OF SCIENCE IN MECHANICAL ENGINEERING

THE UNIVERSITY OF TEXAS AT ARLINGTON

May 2021

Copyright © by Manjunath Hanumantha 2021

All Rights Reserved



Dedication

“Always remember those who believed in us and helped us achieve our goals throughout our journey” -

Words from my parents, dedicating my success to my beloved family.

Acknowledgement

I would like to express my profound gratitude to my supervising professor, Dr. Amir Ameri for his commendable advice, encouragement, continuous support and guidance throughout my graduate study. I am also grateful to Dr. Narges Shayesteh for her valuable guidance and support. Their immense knowledge and prolific experience have galvanized me in all the time of my academic research and daily life. Without their supervision and efforts this thesis would not have been possible.

I would like to thank Dr. Chen Kan and Dr. Agonafer Dereje for providing their time and expertise to serve on the thesis committee. In particular, I would like to thank the Characterization Center for Materials and Biology at the University of Texas at Arlington for allowing us to use their resources to conduct experiments.

I want to thank Mr. Bharath R, at IAM lab for believing in me, supporting me, and leading me through every step of my research work. Dr. James, Mr. Aditya K, and Mr. Samarth R deserve special appreciation for their contributions to the thesis completion and for making this journey memorable.

I would like to thank my mother, Ms. Bhagya L, my father, Mr. Hanumantha B, my sister, Ms. Divya M, and my brother-in-law, Mr. Mahesh V, for their advice, love, and faith in me, as well as my friend, Mr. Shubham R, for his encouragement during my academic journey.

Abstract

STUDY ON THE MICROSTRUCTURAL AND HARDNESS VARIATIONS OF UNSUPPORTED OVERHANGS FABRICATED USING SELECTIVE LASER MELTING

Manjunath Hanumantha, MS

The University of Texas at Arlington, 2021

Supervising Professor: Dr. AMIRHESAM AMERINATANZI

Additive manufacturing is a new manufacturing technology that allows for extreme design freedom as well as the simultaneous production of many parts with high complexities. IN718 is a high-strength, corrosion-resistant super alloy of nickel and chromium. It is ideal for high-end applications such as rocket nozzles and turbines because it can handle exceptionally high pressure and heat. Because of its high stiffness qualities, conventional manufacturing of complex IN718 geometries is challenging. Various fabrication techniques have been developed, and this study focuses on selective laser melting (SLM) because of its potential to produce near-perfect parts at a low cost when working with a variety of different materials. As a result, selective laser melting (SLM) provides a viable solution for the high-accuracy fabrication of IN718 components. One of the drawbacks of this technique is the need for supports to fabricate overhanging structures. These supports must be carefully planned and appear to consume a significant number of resources. Because of the superalloy's high toughness and job hardening, machinability of IN718 is extremely difficult, requiring the use of additive manufacturing, specifically SLM.

The fabrication of complex geometries is difficult without the proper allocation of support to overhang and angled structures for the component, which holds the component intact and maintains structural stability during manufacturing. Multiple properties of SLM components, such as microstructural structure, mechanical properties, stiffness, and toughness, are either directly or indirectly influenced by the allocation of support to overhang and angled geometry.

This research focuses on angled structures made without supports. The overhangs were created with standard process parameters for varying thicknesses. Variations in melt pools and Vickers hardness were determined using microstructural analysis and hardness tests. The results of this study will help us in predicting the need for supports in overhangs and inclined structures used within a complex geometry component.

Table of Contents

Dedication	iii
Acknowledgement	iv
Abstract	v
Table of Contents	vii
List of Tables	ix
List of Figures	x
Chapter 1. Introduction	12
Motivation	12
Objectives	12
Approach	13
Outline	13
Contribution	14
Chapter 2. Background and literature review	16
2.1. Additive Manufacturing processes	16
2.1.1. A brief history of additive manufacturing development	16
2.1.2. AM technologies	17
2.1.3. Effective parameters on AM processed part	24
2.1.4. Advantages and disadvantages of AM	30
2.1.5. AM applications	31
2.2. AM of Inconel718 superalloy	32
2.2.1. Brief introduction to Inconel718 superalloy	32
2.2.2. SLM of IN718	34
2.3. Overhangs constrain consideration in AM of alloys	35
2.3.1. Importance of overhang supports in SLM	36

2.3.2. The effect of overhang on the mechanical properties of as-fabricated parts.	36
Chapter 3. Design, fabrication, and experimental procedures	37
3.1. CAD design.....	37
3.2. Powder preparation and fabrication	39
3.3. Sample preparation	40
3.4. Experimental procedures.....	42
3.4.1. Scanning electron microscopy (SEM) and Energy Dispersive X-Ray Spectroscopy (EDS)....	42
3.4.2. X-Ray diffraction (XRD).....	43
3.4.3. Hardness analysis.....	44
Chapter 4. Results and discussion.....	46
4.1. Microstructure analysis	46
4.2. Compositional Analysis	51
4.3. Hardness analysis	53
Chapter 5. Conclusions and Future Works	55
5.1. Conclusion	55
5.2. Future Work	56
Reference	57

List of Tables

Table 1. Main features of available laser-based powder bed AM processes.	19
Table 2. Composition of IN718 (wt%) [133]......	32
Table 3. different types and geometrical factors (angle-A and thickness T) of the overhang structures.	38
Table 4. Effect of overhang parameters (Angle and Thickness) on the melt pool size and grain structure of as fabricated samples	50

List of Figures

Figure 1. AM processes are classified into three categories based on their feedstock material: liquid-based, solid-based, and powder-based.	18
Figure 2. A schematic representation of a SLM technique. This procedure begins with slicing the CAD model and continues with a three-step process that can be repeated. Step one is to raise the powder platform, step two is to spread powder, and step three is to melt powder according to the CAD file, and so on. The final product is ready to use after the supports and loose powders have been removed.....	21
Figure 3. The impact of the indirect SLS process on metal powder particle size. The loose powder with a polymer binder is depicted in the first figure. The powder is fused, and the component takes form without causing any damage to the metal powder. The following step describes how, after heating, the polymer vaporizes, resulting in a porous part. To reduce porosity, a metal powder with a lower melting temperature is added to fill the gaps [61].....	22
Figure 4. shows the Stochastic exposure strategy in the Laser cusing process.....	24
Figure 5. Hatch angle: 90° on left and 67° on right.	26
Figure 6. (a):The schematic of the staircase effect in layer-based manufacturing processes and (b):The technique to minimize the staircase effect [100].....	27
Figure 7. Balling effect in the fabrication cycle occurs when the energy for the melt pool is insufficient or the laser melting time is insufficient [109].	29
Figure 8. (a) Parallel scanning strategy in one direction, and (b) with a change in direction at alternate scan; (c) scan strategy with several small islands.	29
Figure 9. Titanium medical implants sculpteo [11](left); Gooseneck bracket for Aerospace (right)[121]; world first 3D printed heart (bottom left) [122]; 3D-printed organs breathing new life into bioengineering (bottom right) [123].	32
Figure 10. Inconel 718 Round Bar [134] (left), casting, and powder (middle) and water connector of an Audi W12 engine [135] (right).	33

Figure 11. a) geometrical variations considered in designing the CAD file including A (angle) and T (thickness); b) 3D view of the CAD file	37
Figure 12. EOS M290 metal 3D printer with a fiber 400 W laser in UTA in IAM-Lab.	40
Figure 13. Allied Techcut 4™ Precision Low Speed Saw used for cutting [164].	41
Figure 14. Allied E-PREP 4™ Grinder/Polish [165].	42
Figure 15. Hitachi S-3000N Scanning Electron Microscope in CCMB Lab at UTA.	43
Figure 16. Bruker D8 Advance X- ray diffractometer in CCMB Lab at UTA.	44
Figure 17. LECO LM 300 AT Micro Hardness Tester [166].	45
Figure 18. SEM micrograph and particle size distribution for commercial EOS IN 718 powder.	46
Figure 19. (a) SEM of fresh IN718 powder; (b) table describing percentage composition for each element in the fresh powder; (c) EDS compositions of IN718 fresh powder tested; d) SEM of as fabricated sample; (b) table describing percentage composition for each element in as fabricated sample; (c) EDS compositions of as fabricated sample.....	47
Figure 20. SEM images of melt pool size for a) A75T3; b) A75T4; c) A75T5; d) A75T6; e) A45T4; f) A60T4; g) A75T4; h) A90T4.....	50
Figure 21. XRD image of fresh powder and overhang samples.	52
Figure 22. Vickers hardness results for all 8 overhang samples with varying angle and thickness.....	53

Chapter 1. Introduction

1.1 Motivation

SLM is one of the most commonly used metal Additive Manufacturing (AM) techniques for IN718, and for the fabrication of almost all complex geometries, support structures to overhang structures are needed. However, the use of a support structure increases the surface roughness of an SLM-fabricated part, which increases material consumption, fabrication time, and cost. Because of these factors, the best orientation must be determined in order to reduce the use of support structures on overhang sections. Our study aims to better understand the relationship between microstructural and mechanical properties, as well as how different component orientations can remove or reduce the need for supports. This aids in understanding the component's manufacturability.

In addition to aiding in the manufacturing of the components, there is a significant impact on the fabricated part properties such as microstructural properties, mechanical properties, hardness, roughness, and so on. Since these are sacrificial entities, the material, time required, as well as multiple factors such as energy, argon gas, and so on, result in an increase in direct and indirect costs. As a result, the optimal condition should be recognized, pinpointed, and applied such that these critical economic factors are consumed less.

1.2 Objectives

This research focuses on the influence of various types of overhang geometry fabricated without support structures on hardness, chemical composition, and microstructural behavior such as melt pool and grain structure. Since all of these factors are interconnected, it is known that changes in the overhang thickness and overhang inclination parameter were needed in order to achieve the best results. Although much research has been done on developing a relationship between variation in overhang dimension and microstructural behavior, as well as component hardness, limited work has been done on variation in grain

structure. To gain a clear understanding of how overhangs affect the fabricated component and how overhang parameters can be adjusted to achieve the aforementioned aim.

1.3 Approach

A review of the literature was the first step in starting this study and understanding the basic process and important parameters for SLM manufacturing of IN718 components, the benefits and drawbacks of supports in SLM, the types of overhangs fabricated without support structures, and so on. Following the analysis of the literature, a structured plan for modeling various overhang structures was created. To understand the impact of microstructural behavior on overhang geometry without supports, several iterations of the same parts with different overhang thickness and angle values were created. The CAD designs were created using different software, including Solidworks, Magics, and others. The parts were fabricated on an EOS M290 machine, and after that, they were carefully removed from the build platform. Overhangs were separated from the base part and prepared for various tests such as X-ray Diffraction (XRD), Selective Electron Microscopy (SEM), Vickers Hardness, and so on. At every stage of the process, the utmost safety was maintained, and proper data recording and labeling was ensured. The remaining results were interpreted, and the effect of the overhangs generated without supports for IN718 parts was observed and recorded for scientific purposes.

1.4 Outline

The chapter 1 provides an overview of the study as well as acknowledgement to the scientific community and members for their direct and indirect efforts.

Chapter 2 provides information on the background and literature review. Section 2.1 talks on the history of metal AM and the factors affecting the SLM fabrication method, along with benefits and drawbacks. Subsection 2.2 talks more about the material being used, i.e., IN718, history of the same, and its importance in the metal AM ecosystem. Details on supports and the importance can be obtained from

chapter 2.3. Explanation on the overhang constrains, importance and their effects on the mechanical properties of fabricated part.

Chapter 3 describes the CAD design of the part and the various overhang geometry that is fabricated with variation in angle thickness and angle for the study. In chapter 3.3, a thorough description of the handling and preparation of powder metal is given. In chapter 3.4, the various experimental procedures used in the analysis, as well as the specifics and settings, are listed.

The final work of presenting experimental recordings and the interpretation for multiple criteria is outlined in Chapter 4. Along with the results, images, and descriptions of the component fabrication and overhang conditions are given.

Finally, chapter 5 presents the conclusions with appropriate reasoning and discusses how the community can use this study to achieve the best outcomes for all.

1.5 Contribution

This study's contribution will be in line with the following:

- (i) Determination of the microstructural effect of the overhang structure without supports for IN718 parts by SLM fabrication.
- (ii) Investigation of results for variation in thickness of overhangs without support structure for parts manufactured by SLM.
- (iii) Investigation of results for variation in the angle of overhangs without support structure for parts manufactured by SLM.
- (iv) Study and comparison of various types of samples having variation in overhang thickness and angle fabricated without support structures using SLM technique of IN718 parts.
- (v) Study and determination of effect on melt pool structure for various overhangs condition for IN718 samples fabricated by SLM method.

(vi) Study and Determination of Hardness value for IN718 parts fabricated by SLM process with different types of overhangs fabricated without supports.

Chapter 2. Background and literature review

2.1. Additive Manufacturing processes

Additive manufacturing is the process of building a desired solid part layer by layer which has many advantages over traditional manufacturing process, starting with a CAD file and then approximating it into triangles and slices that represent the information of each layer that will be 3D printed [1, 2]. 3D printing technology in additive manufacturing is well known for its versatility in the fields of rapid prototyping and solid freeform fabrication. Due to its wide range of applications, 3D printing technology is used in human tissues [3, 4], aerospace [5], the next generation of photovoltaic panel materials [6], makeup [7], costumes for movie characters [8], hearing aids, braces for teeth [9], prosthetics [10], toys [11], jewelry [12], and even to decorate pastries at the local bakery [13]. The 3D printing process begins with creating a three-dimensional CAD design of the part with all necessary dimensions, followed by using AM tools such as magics and 3DXpert software to slice the 3D model into thin layers of two-dimensional cross sections. Later, the sliced 3D model data is used to fabricate each layer on top of the previous layer inside the fabrication chamber [14-16].

AM has developed into a mainstream mode of fabrication as a result of ongoing research. AM allows for the manufacturing of a wide range of metallic, non-metallic, ceramic, and plastic-based components. While AM techniques can prove to be more advantageous than traditional methods, there are a number of drawbacks. Some of the benefits include low-cost and small-batch production, the consolidation of an assembly into less number of components, the integration of porous structures, and the ease with which complex designs with internal features can be fabricated [17, 18].

2.1.1. A brief history of additive manufacturing development

AM technology has seen dramatical advancements over the last 20 years. In 1984, Deckard and Beaman started developing a 3D printing technique for powder content, which used a 100W YAG laser as

a heat source [19]. Deckard then developed the 'Betsy' machine in 1986. The research into selective laser sintering (SLS) continued, and a patent was eventually filed at the University of Texas at Austin. [20, 21]. In 1995, EOS introduced the EOSINT M250 for direct metal laser sintering (DMLS). In 1997, EOS and 3D systems worked closely on SLS. [22], and, finally, 3D Systems secured the right to SLS by purchasing the corporation that held Deckard's patents. [19]. In the year 2000, Andersson and Larson invented Electron beam melting (EBM). [23], Arcam then introduced it to the market in 2002. [24]. In January 2010, HP and Stratasys agreed to collaborate on the development of a line of HP-branded 3D printers for Stratasys. [25].

Aside from that, Cornell University and the University of Bath launched two open-source FDM 3D printers, Fab@home and RepRap, in 2004. [26-28]. FDM was the most used technique in earlier printers, but as patents expire, the focus is shifting to SLA. While FDM-fabricated parts are inexpensive, their mechanical properties and performance are substandard. [29]. Despite the high cost of laser-based printing operations, the parts have some superior output characteristics. High-end industrial printers usually come with printer-specific software that aids in slicing the 3D model and delivering precise commands to the 3D printing machine. Commercial 3D printers are available on the market from 3Dsystems and Stratasys who merged with Objet in 2013. [30].

2.1.2. AM technologies

There are different types of 3D printers on the market, including flow-based, powder-based, and solid-based models. Powder-based methods appear to be the most exciting field based on the properties of the manufactured components. (Figure 1). Laminated object manufacturing (LOM) is a type of solid-based process that includes stereolithography (SL) and fused deposition modeling (FDM). After that, powder bed-based processes include selective laser sintering (SLS), laminated engineering net shaping (LENS), and electron beam melting (EBM) [31].

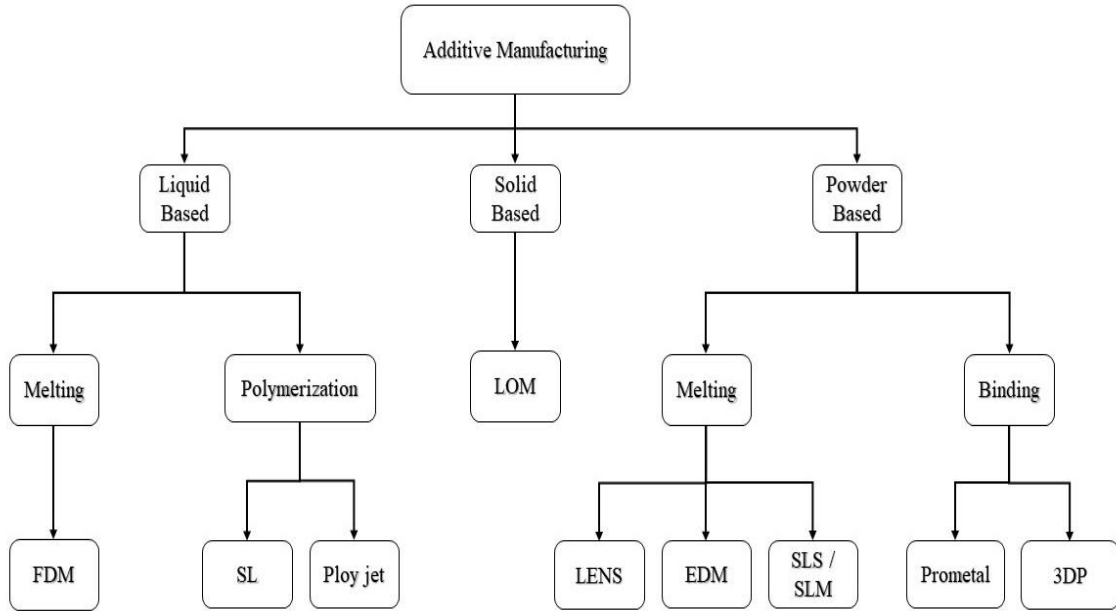


Figure 1. AM processes are classified into three categories based on their feedstock material: liquid-based, solid-based, and powder-based.

The majority of laser-based processes are classified as SLS, SLM, LMA, DMLS, LMS, or SLS/HIP. Several groups have used the aforementioned AM techniques to create parts for real-world applications. Table 1 summarizes numerous articles on laser-assisted manufacturing. There, machine model, laser power, material, layer thickness, scanning speed, and other important terms related to metal AM are discussed.

Table 1. Main features of available laser-based powder bed AM processes.

AM Technology	Machine Type	Laser Power (W)	Scanning Velocity (mm/s)	Hatch Space (μm)	Layer Thickness (μm)	Powder size (μm)	Author
SLM	-	110, 110, 120, 130	600, 400, 400, 400	-	-	15- 45	Jia <i>et al.</i> [32]
EBM	Arcam® EBM S12 machine	-	-	-	50	-	Raghavan <i>et al.</i> [33]
SLM	SLM 250HL machine	100 W	540	120	30	30	W.Tillmann <i>et al.</i> [34]
EBM	ARCAM A2 SEBM System	594 W	2200 to 8800	100, 37.5	-	-	Korner <i>et al.</i> [35]
EBM	EBM 12 SYSTEM FROM ARCAM AB	-	918	-	70	47 \pm 23	Hinojos <i>et al.</i> [36]
SLM	Concept M2 machine	180-220	-	-	30 to 45	-	Lambert, Dennis M [37]
DLD	IPG Photonics 5 kW system equipped with an ABB robot	5000	-	-	-	-	Y.N.Zhang <i>et al.</i> [38]
SLM	SLM 280HL	250, 950	700, 320	120, 500	50,100	20 to 60	V.A.Popovich <i>et al.</i> [39]
LAM	-	550	-	-	-	-	Yuan Tian <i>et al.</i> [40]
SLM	DMP PROX300	450	1000 to 1800	50 to 90	70	5 to 25	K.Moussaoui <i>et al.</i> [41]

2.1.2.1. Selective laser melting process

Selective laser melting (SLM) has its versatility in feedstock and shapes and emerged as the most promising AM technology. This process can accurately produce complex components with high dimensional accuracy and good surface integrity without the need for post-processing on fabricated pieces, which traditional processes cannot easily keep up with [42-47]. SLM processes include layer-by-layer SLM of pre-spread powders to produce a three-dimensional dense component directly from user-defined CAD data [48-54].

A schematic of a generic powder bed SLM device is shown in Figure 2. Raking powder around the work area is the first step in the SLM process. An energy source, such as an electron beam or a laser beam, is designed to provide the required amount of energy to the bed's surface in order to melt or sinter the metal powder into the desired form. To produce a sturdy three-dimensional portion, more powder is raked over the work area, and the procedure is repeated. SLM has the capacity to create high-resolution features, internal passages, and retain dimensional control [55-58]. The required microstructures of SLM-processed parts are invariably influenced by complicated physical and chemical interactions within the molten pool, which are frequently the result of the laser's non-equilibrium processing technique [59].

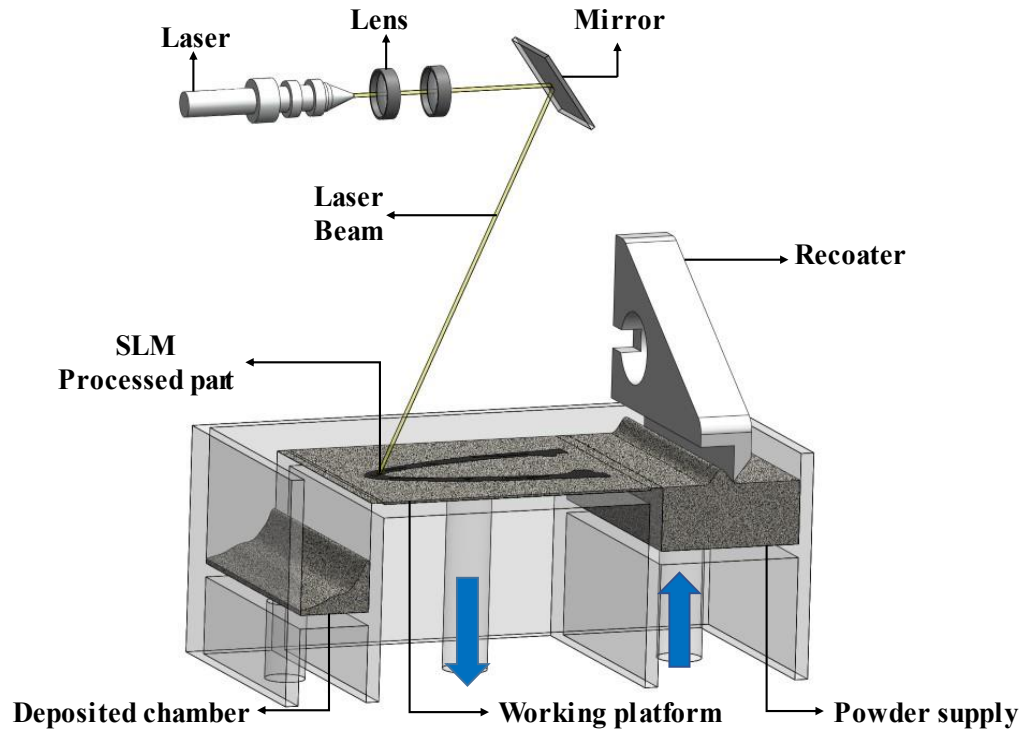


Figure 2. A schematic representation of a SLM technique. This procedure begins with slicing the CAD model and continues with a three-step process that can be repeated. Step one is to raise the powder platform, step two is to spread powder, and step three is to melt powder according to the CAD file, and so on. The final product is ready to use after the supports and loose powders have been removed.

2.1.2.2. Selective laser sintering

The two major types of selective laser sintering are direct and indirect (SLS). Sintering refers to the fusion of powder particles at high temperatures without melting. The powder melts partly in direct SLS, resulting in a low packing density. Direct SLS has a sufficient sintering density but results in cracks due to thermal stresses. Preheating the powder bed with a diffused CO₂ laser up to 1700 °C is one realistic solution. The part's maximum height is 3 mm [59]. As per Figure 3, the green portion of indirect SLS is obtained by melting a binder phase. Following that, the green element is turned to ceramic by rebinding and furnace heating. The lack of binder content in direct SLS is a significant contrast between it and indirect SLS [60].

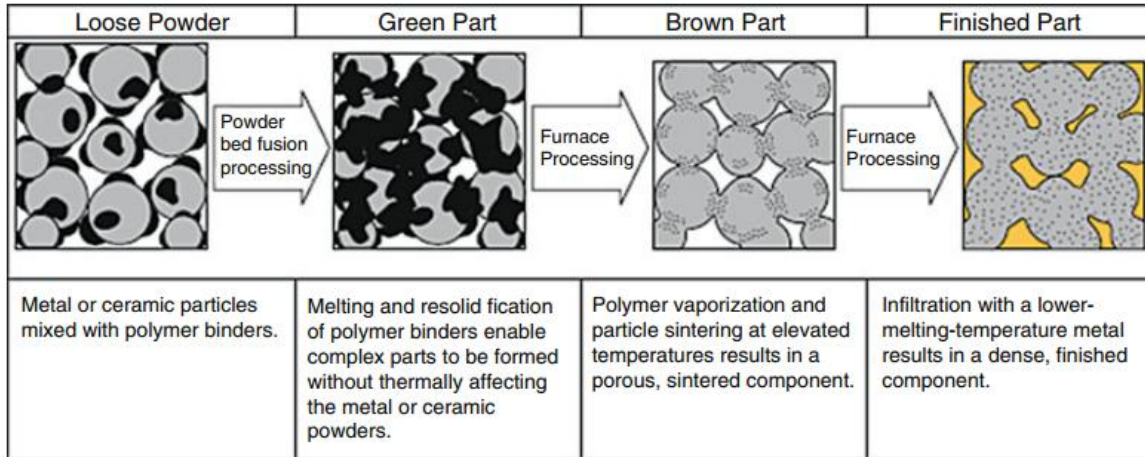


Figure 3. The impact of the indirect SLS process on metal powder particle size. The loose powder with a polymer binder is depicted in the first figure. The powder is fused, and the component takes form without causing any damage to the metal powder. The following step describes how, after heating, the polymer vaporizes, resulting in a porous part. To reduce porosity, a metal powder with a lower melting temperature is added to fill the gaps [61].

2.1.2.3. Direct metal laser sintering

Due to various recent advancements, the original requirement for binder for titanium and aluminum has been removed, and the ability to produce fully functional metal prototypes has improved. Under the right conditions, this process will produce parts with the same or nearly identical properties as a conventionally fabricated component. The ability to create more complex parts in a single phase is an advantage over SLS, but it has drawbacks such as high internal tension and component distortion, which leads to a rise in temperature gradient and densification ratio, and poor surface finish due to balling and dross forming [62-64]. The surface finish of a component is important in many applications, such as those that need a surface roughness of 0.8 μm or better to prevent premature loss from surface-initiated cracking. Direct metal laser sintering shows great potential for direct production of functional prototypes and tools as compared to other rapid prototyping technologies [65].

2.1.2.4. Laser micro sintering

In 2003, the Laser Institute Mittelsachsen eV developed laser micro-sintering. 3D-Micro-mac AG, Chemnitz, Germany, patented this technique and facilities, which offered a resolution of less than 30µm and less roughness ($R_a = 1.5 \text{ V}$). The powder content is alternately coated and sintered by a laser beam scanning the cross section of the intended sinter part in selective laser sintering [66]. The production process flow for laser micro sintering is similar to SLM, except it provides a higher resolution for parts than SLS, which is less than 100 µm [67]. Another advantage of this approach is the reduced strain in the sections caused by the q-switched Nd: YAG-laser pulse [68].

2.1.2.5. Laser cusing process

M1 cusing, M2 cusing, M2 cusing multi-laser, and M3 linear devices were introduced by Concept Laser. Cusing is a combination of the letter "C" and the word "Fusing." The 'stochastic exposure technique,' in which each layer is referred to as an island, was a distinctive characteristic of this system (Figure 4). This method reduces internal stress in the fabricated component [69]. The typical layer thickness for this process is 20 to 50 µm. [70]. M2 cusing is the second generation of this technique produced by concept laser. M2 cusing is fitted with a double-fiber laser, which reduces fabrication time. The M3 linear machine is simpler to use because of the material versatility, which includes stainless steel and other chromium alloys. Nonferrous alloys, such as titanium (Ti6AlV4), aluminum (AlSi12 and AlSi10Mg), and other cobalt-chrome and nickel-based alloys, can be processed [56, 57, 71-77].

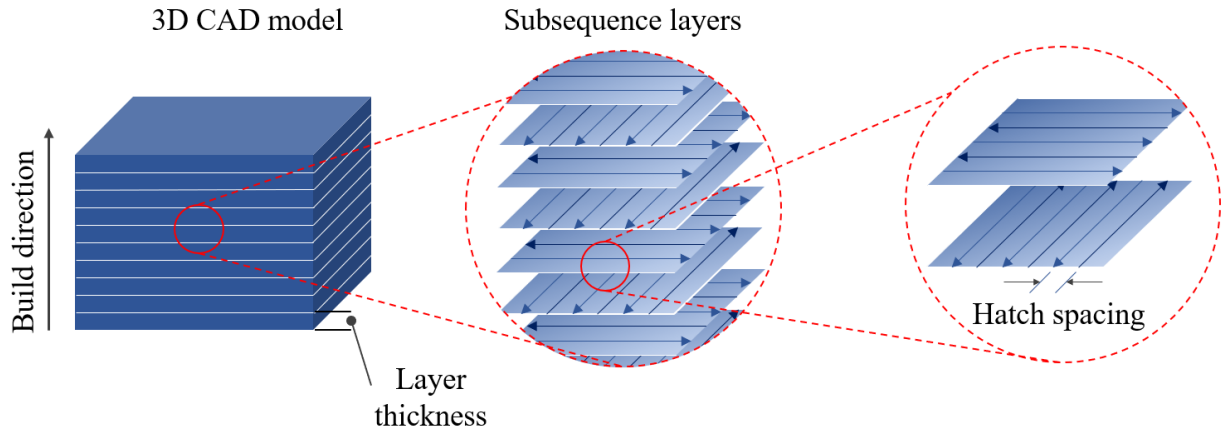


Figure 4. shows the Stochastic exposure strategy in the Laser curing process.

2.1.3. Effective parameters on AM processed part

AM is dealing with the interpretation of interactions between various parameters related to system and materials, both directly and indirectly. Powder particle size, scanning technique, laser strength, hatch spacing, and other parameters must be adjusted and supplemented based on the component specifications [78-80]. Yadroitsev *et al.* [81] introduced process parameters distinguished as the following factors: (i) Manufacturing strategy: component orientation and support strategy. (ii) Laser parameters include laser intensity, spot size, and scanning velocity. To summarize, factors such as powder morphology, laser strength, hatch size, layer thickness, scanning velocity, and scanning strategy are the primary focus for optimizing part quality. Since all of the process parameters are interdependent, it is critical to identify an optimal value that satisfies the criteria and provides the optimal build quality [82, 83]. For SLM to fabricate a full-density sample, an optimal combination of these processes is needed [55, 58, 84-92]. Equation 1 can be used to measure the laser energy density from laser processing parameters [93-95]:

$$\text{Laser energy density} = \frac{\text{Laser Power}}{\text{Scan Spacing} \times \text{Scan Speed} \times \text{Layer Thickness}} \quad \text{Equation 1}$$

The initial feedstock material influences heat capacity and latent heat. Insufficient energy occurs when the combination of laser strength, scanning speed, and layer thickness is inadequate. This problem causes balling, which is caused by the wetting of the molten pool in relation to the other sheet [96]. Low

scanning speeds and high laser power cause excessive material evaporation and the key-hole effect [97]. Not just that, but inadequate hatch spacing causes the parts to become more porous. The laser window becomes blocked due to the condensation of the volatilized material in the fabrication chamber, reducing the laser intensity. Due to vaporization in SLM, the above parameters are affected [98].

2.1.3.1. Powder particle morphology

Powder atomization, particle size, and shape affect the density and mechanical properties of SLM components, according to Irrinki *et al.* [98]. Attar *et al.* [99] investigated the influence of powder morphology on the density of *in-situ* Ti-TiB composite components, finding that the density of samples fabricated with spherical and irregular particle shapes was 99.5% and 95%, respectively.

2.1.3.2. Laser power and spot size

The property of laser power affects the melting of feedstock material, which is governed by AM. The melting phase of powder and its properties degrade as laser intensity increases. As a result, based on the type of material, an optimal level of laser power should be determined. 5 watts is sufficient for polymers, but 500 watts is needed for ceramics and metals. A typical commercial SLS or SLM machine has a laser power of 50 to 400 W. The laser spot size is another factor to consider when determining laser intensity. Higher laser density is achieved with a smaller laser spot size, which contributes to adaptation for use with materials with a higher melting point [100].

Laser beam diameter is a term for the size of a laser spot. The diameter of the laser spot size is depicted by the point at e^{-2} for the laser peak strength of a pulse for a Gaussian wave. It has an effect on energy density, accuracy, and processing speed. The spot size is inversely proportional to the energy density. It is necessary to determine the minimum spot size requirement, the wavelength, and the laser's quality [101]. It's clear that small spot sizes are used to create thin walls and small holes. However, this increases the build time, which is not always desirable. Thus, thin boundaries are used for small features, whereas larger spot diameters are used for bulk production [100].

2.1.3.3. Hatch spacing

The distance between the centers of one beam and the center of the adjacent beam can be calculated to determine the separation between two tracks, also known as hatch spacing, scan spacing, or hatch distance [100]. The hatch spacing and the production speed have a significant correlation. Less hatch spacing reduces the laser's scanning time, and vice versa. Hatch angle θ , which is the angle between the laser scanning direction among the successive layers, is another important parameter. When the hatch angle is 90, the alignment of the melted rows will be the same after four layers, i.e., the first one [102].

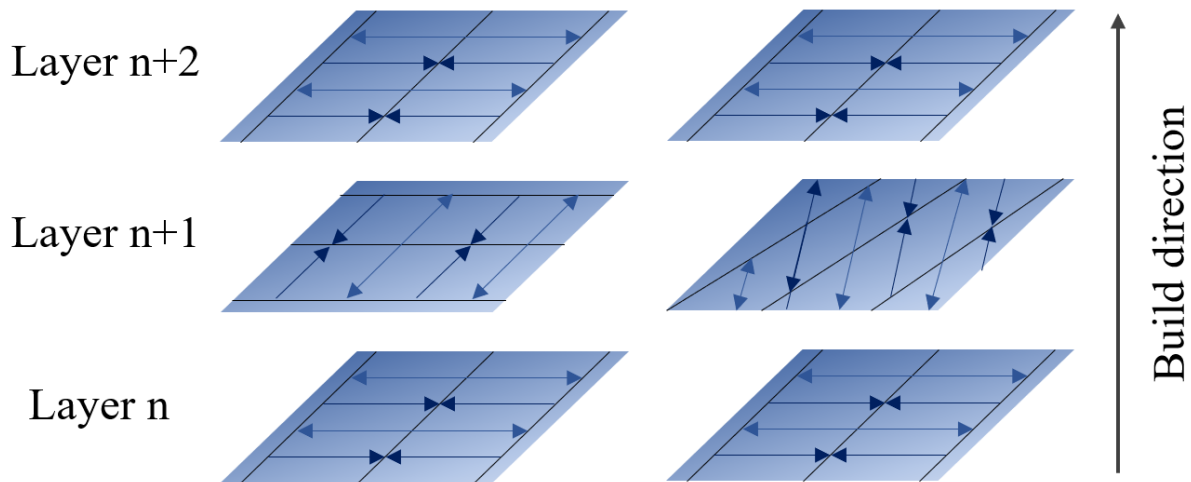


Figure 5. Hatch angle: 90° on left and 67° on right.

2.1.3.4. Layer thickness

A layer thickness refers to the thickness of a powder layer or a CAD slice. Fabrication speed, build time, and layer thickness are all directly proportional. However, as the layer thickness increases, the quality of the AM-processed component decreases. In AM, a thick fabrication layer may cause problems. An increase in layer thickness is associated with higher laser energy. Thinner layers, which have less shrinkage and distortion, can be used to improve the dimensional precision of the components. Although thin layers have several advantages, there is a direct increase in build time and expense. Instead of using higher laser energy, two scans with lower energy can be chosen for better component properties for a thick layer [100]

The thickness of an AM layer is determined by the sample's topology. As seen in Figure 6a, curved objects cannot be fabricated layer by layer since there would be gaps on the sides of the component [100]. This is known as the staircase effect. As a result, to remove undesirable features such as the staircase effect, the layer thickness must be optimized. As a result, higher layer thicknesses can be assigned to vertical surfaces, but thinner layers are recommended for angled surfaces, as seen in Figure 6b.

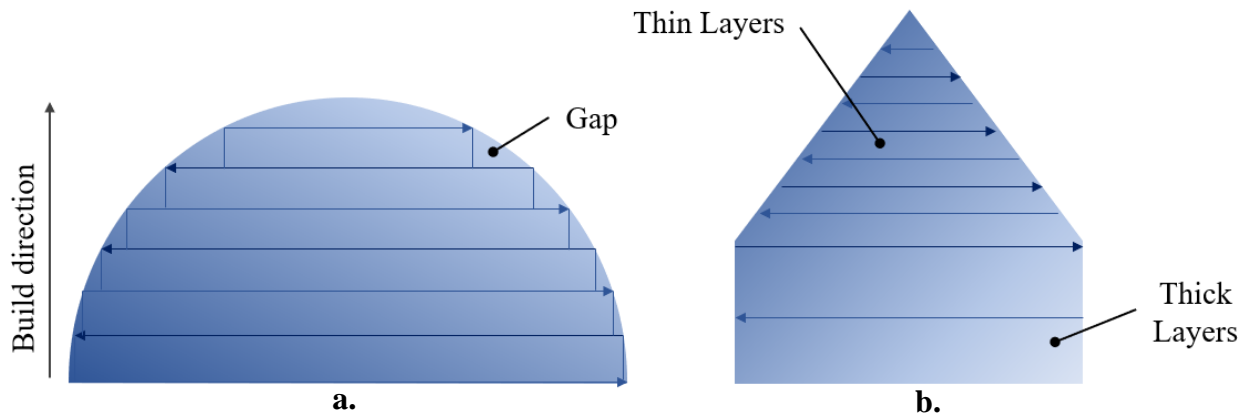


Figure 6. (a):The schematic of the staircase effect in layer-based manufacturing processes and (b):The technique to minimize the staircase effect [100].

2.1.3.5. Scan speed

The scanning speed is the rate at which a laser beam scans a line, and it influences the rate of production, as well as the production speed and building time. If the scanning speed increases, the laser energy density decreases and becomes inadequate for proper melting of the material. A rise in laser power, on the other hand, would help to compensate for the problem. Higher scan speeds do not allow the layers to solidify until the next layer, which influences the melt-pools. Higher scanning speed would result in longer and thinner melt-pools, which is undesirable since the likelihood of breaking into smaller pools (balls) is high, according to the principle of Rayleigh Instability (Figure 7) [100, 103].

2.1.3.6. Scan strategy

Scanning strategy refers to the process of scanning a powder bed with a laser beam to increase build speed and component quality. The use of an optimized scanning technique reduces distortion, warp, inaccuracy, and porosity [104, 105]. The scanning strategy is divided into two main types: fill scan and contour scan. In an infill scan, the whole region is scanned, while a contour scan just scans the borders. An interpretation of the fill scan and counter can be derived from Figure 8a. The fill scan scans the entire region in one direction. Figure 8b depicts another scanning strategy with an alternating search path for fill scanning. The scan time in Figure 8b is less than that in Figure 8a. This is due to the fact that in Figure 8a, the laser must return to the starting point of the previous layer, as compared to the other strategy, which uses continuous scanning. Parallel lines scan modes for SLS/SLM are simple to program and use. Though scanning can be done in both horizontal and vertical directions, a consistent scanning angle can be assigned. A consistent scanning strategy reduces shrinkage, residual stress, and anisotropy [100, 106]. Shrinkage stress can cause warping and distortion of the component [107]. As seen in Figure 8c, the plane can be separated into smaller islands, which can reduce anisotropic buildup. As a result of separating and scanning the plane by islands, the issue of heat accumulation is reduced from a larger area (the whole region) to a small area (an island). Specific scanning strategies for different layers may be used to target non-uniform heat distribution. After scanning an island, the next scanned island is at the opposite end of the plane to reduce the buildup of tension, which causes warping of AM-processed parts, especially overhangs. Another factor is that if the scanning path is longer and shorter, the layer can split into many balls due to Rayleigh instability (Figure 7). As a result, a scanning strategy involving several islands is preferable [100, 103]. Different scan strategies such as stripes, custom, chess, and flow-optimized scan strategy has a effect on the microstructure and mechanical properties of fabricated Specimen[108].

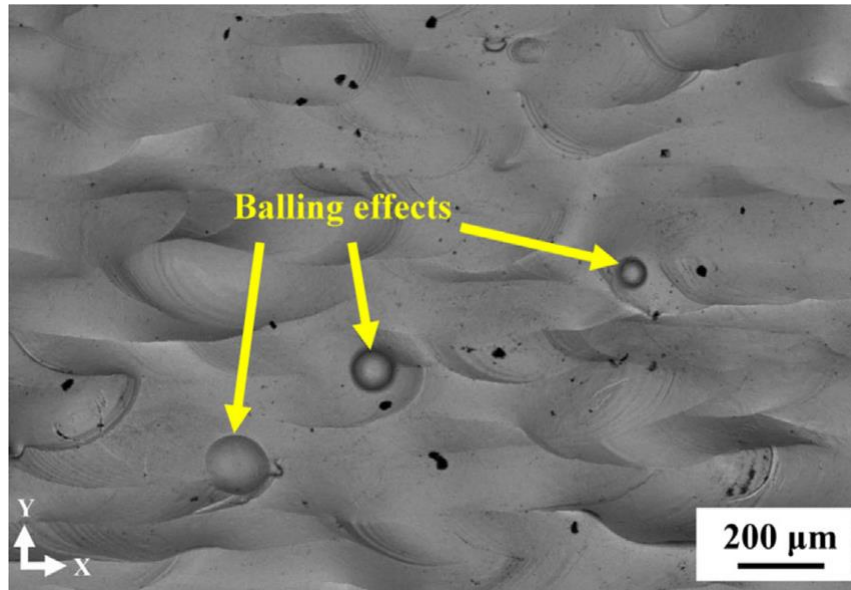


Figure 7. Balling effect in the fabrication cycle occurs when the energy for the melt pool is insufficient or the laser melting time is insufficient [109].

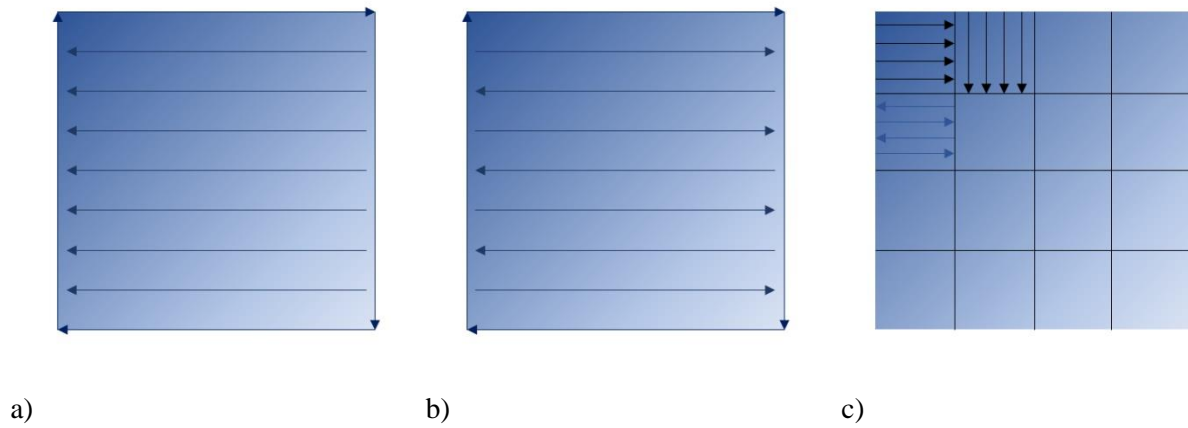


Figure 8. (a) Parallel scanning strategy in one direction, and (b) with a change in direction at alternate scan; (c) scan strategy with several small islands.

2.1.4. Advantages and disadvantages of AM

AM is extremely important in the industry. Several factors, including reduced build time, human interaction, and product development cycles, are among the major benefits, as is the unrestricted ability to produce complex components. [110]. There is progress in the technology securing a significant role in the future of the manufacturing industry due to an ever-increasing development in the AM field, as well as promising progress and rapid industrial adaptations. [31]. The main objective is to produce parts and designs for direct applications.

As the cost of production, product development costs, cradle to grave costs, and others prove to be beneficial over a set of the product manufacturing cycle, AM may have wide-scale adoption in industries. AM's focus is to enhance the economic, environmental, and experience importance of its products. Though it cannot be specifically quantified, the ability to manufacture in-house parts, maintain product security, and privacy will all contribute to profitability. [111-113]. In situations where the complexity of the component is high and the output volume is limited, the lack of a tool contributes to a decrease in direct production costs. [114]. As a result, the fabrication process and time to market for such complicated parts can be greatly decreased. Just as a coin has two sides, there are many problems involved with AM-processed components, and there is a need for improvement in AM before they can be considered a standard in the manufacturing industry.. All of these advances are the removal of the need for surface finishing. There is no consistency in the overall surface finish of the component due to the need of support removal. This is undesirable in high-end applications where the surface finish must be flawless. In addition, because of the layer-by-layer construction, the presence of the staircase effect results in an uneven and poor surface finish. These matters would be brought to light in order to improve the properties.

At the moment, AM cannot be used in high-end applications where the error percentage would be close to zero. Nonetheless, it should be remembered that this technology is being rapidly embraced by scientists, medical practitioners, students, artists, and a variety of other individuals. [115-117].

2.1.5. AM applications

Along with extensive studies, proof of substantial advancement may be concluded with a growing number of applications in and not limited to aerospace, industrial, academia, biomedical, and energy [118]. Alternative applications include the design of structural plans for construction, jewelry prototypes, and apparel. 3D printing is now having an effect on the food industry [119]. Not just that, but patient-specific models of the affected body parts are used to better understand the anatomy and schedule the surgery. AM is used by artists to construct a scaled image of their work [2]. Aerospace and car manufacturers use 3D printing extensively due to the ability to produce complex components, while AM is aligned with the medical field in a way where 3D printing of stem cells has recently been adopted and is being produced [120]. Figure 9 shows many commercial implementations of AM.

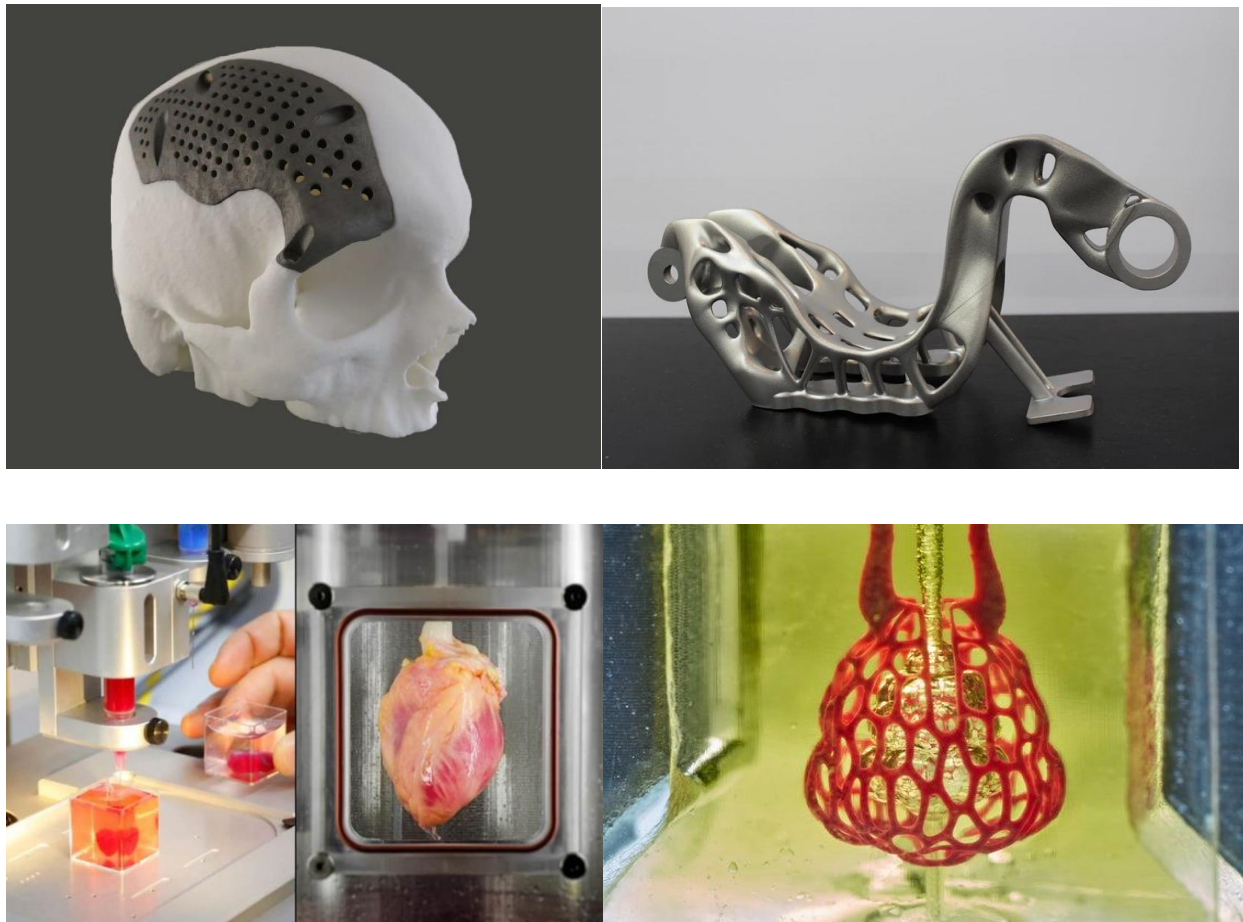


Figure 9. Titanium medical implants sculpted [11](left); Gooseneck bracket for Aerospace (right)[121]; world first 3D printed heart (bottom left) [122]; 3D-printed organs breathing new life into bioengineering (bottom right) [123].

2.2. AM of Inconel718 superalloy

2.2.1. Brief introduction to Inconel718 superalloy

The need for a durable solution strengthened non-hardenable alloy for high-end applications at 1200 to 1400°F (650 to 760°C) paved the way for the development of Inconel718 (IN718). Stability was regarded as a critical requirement in the early stages of production for Ni-based superalloys. It was crucial to retain the standard, so screening tests were implemented to verify the age-hardening reaction and metallurgical stability. After some period, the production of IN718 superalloy fulfilled the search. IN718 superalloy is an age-hardenable Ni-Cr austenitic alloy with a work temperature range of 257 °C to 704 °C. [124, 125]. Corrosion resistance is aided by the crystallization of Ni and Cr in γ phase. The precipitation of Ni₃Nb into the γ ” process leads to the alloy's hardening [126, 127]. Although these features are ideal for critical applications, they make casting, forging, and other traditional metal processing methods challenging [128]. The surface quality of the finished component is improved by reducing burr forming and increasing machining precision, all of which require High Speed Machining (HSM). IN718 production began in 1960 with the aim of integrating improved mechanical properties, creep-rupture strength, tolerance to chlorine and sulfide stresses and corrosion, intense temperature resistance, oxidation resistance, welding characteristics, and post welding cracking resistance, resulting in IN718 being one of the most used Ni-based superalloys. Because of these features, IN718 can be used in aircraft engines, turbine blades, combustion chambers, and nuclear reactors. [129-132]. Table 2 shows the chemical composition of commercial IN718.

Table 2. Composition of IN718 (wt%) [133].

Element	Wt%
Nickel	50.00-55.00
Chromium	17.00-21.00
Iron	Balance
Columbium	4.75-5.50
Molybdenum	2.80-3.30
Aluminum	0.20-0.80
Titanium	0.65-1.15
Manganese	0.35 max.
Silicon	0.35 max.
Boron	0.006 max.
Carbon	0.08 max.
Niobium	5 max



Figure 10. Inconel 718 Round Bar [134] (left), casting, and powder (middle) and water connector of an Audi W12 engine [135] (right).

Wrought, powder cast, and metallurgy are some general superalloy types. They are capable of providing sufficient mechanical and microstructural properties. [136-138]. Figure 10 depicts various methods of manufacturing IN718. Because of the solid-solution reinforcement and precipitation

strengthening, this material has superior mechanical properties over a wide temperature scale. Meanwhile, traditional machining of IN718 is difficult due to its high hardness, 372 HV for wrought IN718 based on AMS 5663 and 350 HV for cast IN718 based on AMS 5383, and poor thermal conductivity of 11.2 W.m-1.K-1, which will result in significant tool over-wear and unsatisfactory workpiece surface integrity [139]. High dimensional accuracy can be achieved due to the major advantages and superior properties, and hence the demand is higher. [140, 141]. Despite the fact that the benefits of such materials are numerous, there is a need for a non-traditional way of manufacturing, and therefore AM plays an important role in this situation. [59].

In general, nickel-based superalloys are natural AM candidates for both SLM and EBM processes. This condition occurs as a result of the difficulties and limitations of traditional production processes, such as segregation, limited workability, and high machining costs. SLM now manufactures Ni superalloy materials such as IN718, IN625, Hastelloy C, Nimonic 263, and others with low Ti and Al concentrations. IN939, IN100, IN738LC, CM247LC, and Rene 142 are some of the other materials being studied and used.. SLM research has shown significant potential for use in the mainstream manufacturing industry for the fabrication of complex geometry in the shortest amount of time and with the best properties [142].

2.2.2. SLM of IN718

SLM has been identified as a promising non-conventional AM technique with extreme versatility in feedstock, shape, geometry, and achieving high precision and surface integrity. SLM of Ni-based superalloys are mostly used in aircraft engines as swirlers in combustion chambers, which aid in minimizing smoke generation and flame stabilization. It is also used in patching, gas turbine motors, and turbo-charged rotors. [143-145]. Some advantages include excellent corrosion resistance, high temperature strength, fatigue resistance, wear resistance, and weldability. [141]. In their analysis, Lu et al. stated that Fraunhofer ILT and the MCP company used SLM to create complex turbine blades with high surface quality and dense microstructure. [146].

SLM, let alone other manufacturing processes, can produce a wide range of variations in microstructure, hardness, and mechanical properties [142]. Because of its excellent creep properties, tensile strength, rupture strength, and other properties, it can be used in nuclear reactors and liquid-fueled rockets.[147]. Furthermore, its excellent oxidation resistance and hot corrosion resistance have made it ideal for operating at temperatures of 700 °C and environments that are particularly carburizing and oxidizing. [129-131]. Thus, laser-based AM techniques have a wide range of uses for IN718 in the manufacturing sector, with a particular focus on aerospace [148].

However, there are some difficulties in fabricating IN718 using the SLM technique. It has been stated that the IN718 SLM-processed component contains a certain percentage of porosity (relative density 98.4 percent) [59]. Not just that, but there are several other issues, such as unmelted powder contents. [149]. To some point, hot isostatic pressing (HIP) will solve these issues, but the grain size would also coarsen. [150]. To achieve efficient fabrication, an understanding of powder bed fusion limiting factors, such as production quality and component dimensions, should be investigated [151].

2.3. Overhangs constrain consideration in AM of alloys

Overhang structures are outward protrusions in a 3D model that normally stretch past the previously processed layer. While SLM provides a high degree of geometrical flexibility, overhang structure in a target part requires special attention for effective fabrication. Overhang supports are used in powder bed fusion fabrication to build parts and conduct energy from the melt pool to the build plate, which aids in providing stable thermal conditions for the SLM operation. Jingchao Jiang *et al.* [152] worked on understanding the importance of support structures in AM and proposed it as a critical parameter for an effective fabrication of part.

Supports minimize deformation in parts while still performing other tasks such as heat removal and sample fabrication. Though supports are necessary, implementing them would require a significant amount of resources, and creating suitable supports could be tedious and time consuming.

2.3.1. Importance of overhang supports in SLM

Material consumption, energy consumption, and manual post-processing have been identified as effective parameters for the production and removal of support structures in AM by Jingchao Jiang *et al* [152]. According to *Gan and Wong et al* [153] the alignment and distribution of support structure with respect to the part would have an effect on the levelness of the build of parts.

Although the supports are sacrificial, they are an essential function in the SLM process, and good design technique can help reduce them, since they are responsible for a lot of material and energy consumption factors. They are, however, often used to conduct the necessary critical functions [154] such as separating the part from the platform, anchoring the overhanging and floating parts introduced during the build to the platform [155], by dissipating heat away from the newly melted surface and ensuring consistent thermal conditions in the consolidation zone, prevent part curling or distortion caused by thermal stresses [156]. In addition, supports have an effect on roughness, mechanical properties, material use, and microstructural properties. Additionally, to remove the supports, postprocessing procedures are necessary, and surface smoothing processes are recommended for the part [157].

Aside from the numerous advantages, various factors such as internal stress, mechanical properties, material consumption, detachment of parts from building plates, and the maximum height of a fabricated part with total aspects help one understand the effect of geometry on the production ecosystem [158]. Excessive supports result in increased material consumption, build time, and removal time, along with a few other things etc. They have studied the failure of parts because of the weak supports during fabrication. [154].

2.3.2. The effect of overhang on the mechanical properties of as-fabricated parts.

Overhanging features of parts are those that are branches to the main component body with no clear relation to the build plate. The overhang structure or the inclined geometry have a significant effect on the SLM fabricated part [159]. Tolosa *et al* [160] investigated the variation of tensile properties for inclined

samples fabricated with a base geometry in the Z-X to Z-Y plane and the main axis of the sample angled with respect to the z direction. Tensile tests conducted on inclined samples fabricated at various angles with supports revealed that the 45° angle had the highest strength properties. In the SLM process, the majority of the part's sections are attached to the build plate at the bottom, which helps stabilize and keep down the first few layers until the fabricated part body is strong enough to withstand the thermo-mechanical stresses [161, 162]. Mechanical stresses, on the other hand, have a significant impact on overhanging features since there is no underlying stable base to protect them [163].

Chapter 3. Design, fabrication, and experimental procedures

3.1. CAD design

The samples under study were modeled in Solidworks 2019 software (version 2018-2019, Dassault Systems, USA). Samples were built in the form of a corner angled bracket, but with varying plate thicknesses and angle on either side of the angled corner. The design's base area was set to 10×5 mm, with a base thickness of 2 mm for all samples.

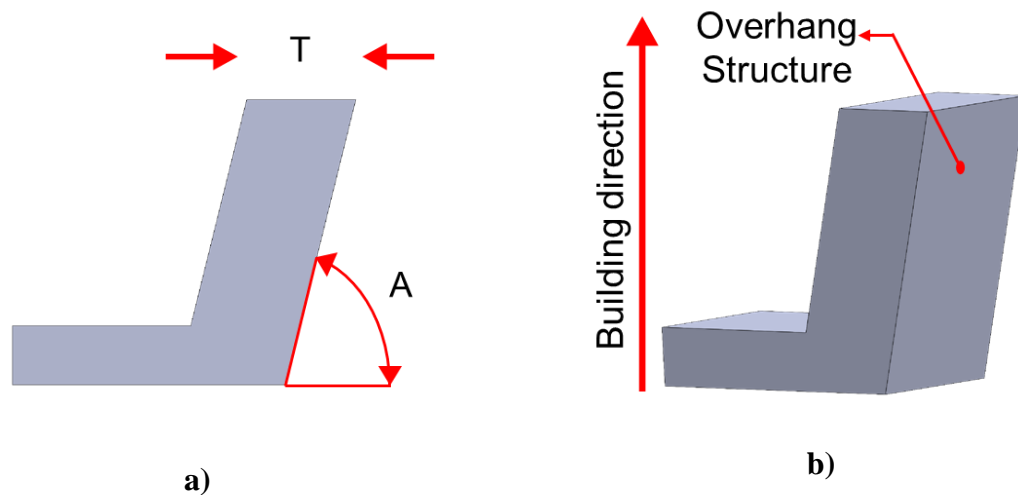









Figure 11. a) geometrical variations considered in designing the CAD file including A (angle) and T (thickness); b) 3D view of the CAD file

Four samples were created with a steady overhang angle of 75°, but their thickness ranged from 3 mm to 6 mm. Moreover, another four samples were created with a steady thickness of 4 mm and different overhang angles of 45°, 60°, 75°, 90°. Table 3 lists corresponding 8 sample names, various geometrical combinations, including variation in angle (A) and thickness (T), were considered in the design models.

Table 3. different types and geometrical factors (angle-A and thickness T) of the overhang structures.

Sample number	Symbol	Overhang structure	Angle (degree)	Thickness (mm)
1	A75T3		75	3
2	A75T4		75	4
3	A75T5		75	5
4	A75T6		75	6
5	A45T4		45	4
6	A60T4		60	4
7	A75T4		75	4



3.2. Powder preparation and fabrication

EOS Engineering Inc. supplied the IN718 powder (Austin, TX). To prevent inhomogeneity in the particle size distribution during fabrication, the powder was sieved with a mesh size of 90 μm . All eight samples with varying overhang thicknesses and angle were created using a DMLS EOS M290 metal 3D printer (EOS GmbH Electro Optical Systems, Germany) fitted with a 400 W Ytterbium fiber laser. The manufacturer suggested the laser processing parameter collection that was used for fabrication. These laser processing parameters were 285-Watt laser power (P), 960 mm/s scanning speed (v), 110 μm hatch spacing (h), and 40 μm layer thickness, with an energy density of 67 J/mm^3 derived from equation 2.

$$E = \frac{P}{h \cdot v \cdot t}$$

Equation 2



Figure 12. EOS M290 metal 3D printer with a fiber 400 W laser in UTA in IAM-Lab.

3.3. Sample preparation

To prepare fabricated samples for the experimental procedure, samples were extracted from the build plate with a bandsaw. After removing the component, an Allied Techcut 4 precision cutter (Allied High-Tech, Compton, CA) (Figure 13) was used to cut the main sample and separate the base area through a plane parallel to the building direction.

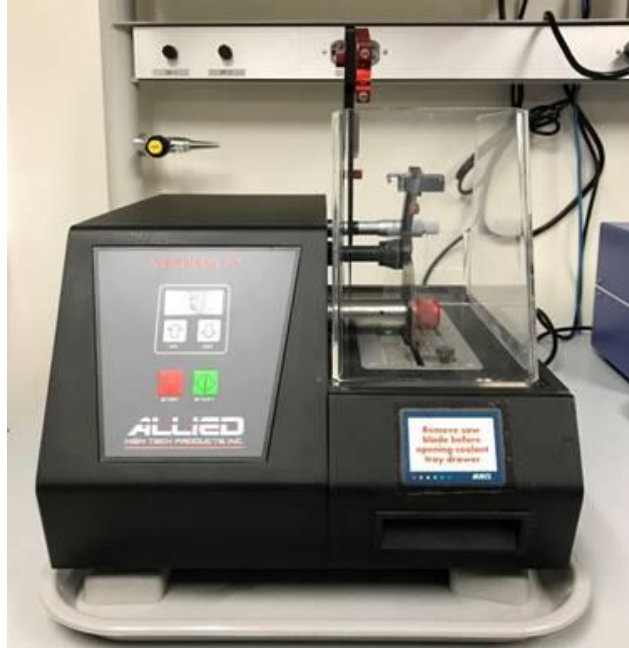


Figure 13. Allied Techcut 4™ Precision Low Speed Saw used for cutting [164].

The cut sample's side surface was set in epoxy resin and polished with an Allied E-PREP 4™ Grinder/Polish machine from Allied High-Tech Products, Inc., Compton, CA, as shown in Figure 14. To maintain consistency in the parts being prepared for SEM investigation, a standardized polishing technique was used. The E-prep 4™ polisher was used in combination with polishing sandpaper of grits 180, 320, 600, 800, and 1200 to achieve the initial polished surface with water as a lubricant. Each polishing cycle was repeated twice for a total of 10 minutes. Following this standard method, a 'DiaMat' polishing cloth with 1 μm polycrystalline diamond suspended solution was used, and a 'Red Final C' polishing cloth with 0.5 μm colloidal silica solution was used. The aim of this procedure was to eliminate material removal deformations. Both the 'DiaMat' and 'Red Final C' polishing cloths had a 10-minute time span. Before each cycle, the machine parts and samples were washed with distilled water and blown clean with compressed air to remove any debris.



Figure 14. Allied E-PREP 4™ Grinder/Polish [165].

3.4. Experimental procedures

3.4.1. Scanning electron microscopy (SEM) and Energy Dispersive X-Ray Spectroscopy (EDS)

A Hitachi S-3000N scanning electron microscope (SEM) was used at the University of Texas at Arlington's Characterization Center for Materials and Biology (CCMB-UTA) to test the sides of the overhang samples on the microstructure of the fabricated main parts (Figure 15). The machine was a PC-controlled variable pressure SEM capable of switching between high vacuum and variable pressure modes.

A PC was used to power and track the SEM setup, which could switch between a high vacuum with a resolution of 3.0 nm and a low vacuum with a resolution of 4.0 nm. The computer, which was connected to a NORAN 7 integrated EDS/EBSD device, had a high-density frame memory of 1280 x 960 pixels. The machine operated at 20kV in the backscatter electron emission modes. The device was equipped with an energy dispersive X-Ray spectroscopy (EDS) module. The purpose of doing EDS was to determine the elements available on the fresh powder as well as the main parts. SEM imaging was conducted on all 8 main samples near the support zone (on the polished side surface).



Figure 15. Hitachi S-3000N Scanning Electron Microscope in CCMB Lab at UTA.

3.4.2. X-Ray diffraction (XRD)

The composition of fused metal was calculated using a Bruker D8 Advance X-ray diffractometer (Figure 16) at CCMB-UTA to determine the crystal and compositional structures of fresh powder as well as the surface of overhang fabricated samples. The X-ray source was Copper (Cu) k-alpha, and the measurements were carried out at room temperature with a wavelength of 1.5406 \AA , phase intervals of 0.02 and in 2θ between 30° and 100° at a speed of 1 s/step .



Figure 16. Bruker D8 Advance X- ray diffractometer in CCMB Lab at UTA.

3.4.3. Hardness analysis

Fabricated components were used to test the effect of various overhang thicknesses on the Vickers hardness of SLM samples. The testing was performed out with 500 g loads applied for 10 seconds. To provide a detailed report on the average hardness value for each sample, at least three indentations were performed.



Figure 17. LECO LM 300 AT Micro Hardness Tester [166].

Chapter 4. Results and discussion

4.1. Microstructure analysis

Figure 18 shows a SEM picture of fresh powder. According to the picture, the powder had a spherical shape, adequate flowability and packing density, a low impurity content, and excellent transformation ability. Furthermore, the image was used for further study of the particle size distribution using ImageJ software [167]. According to the report based on SEM image analysis, an average particle size of 38 μm was identified.

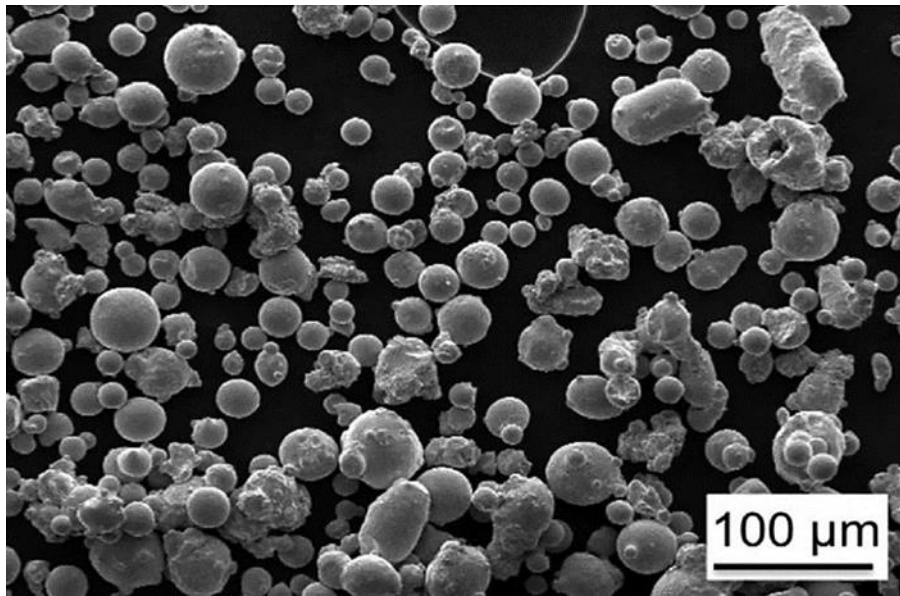
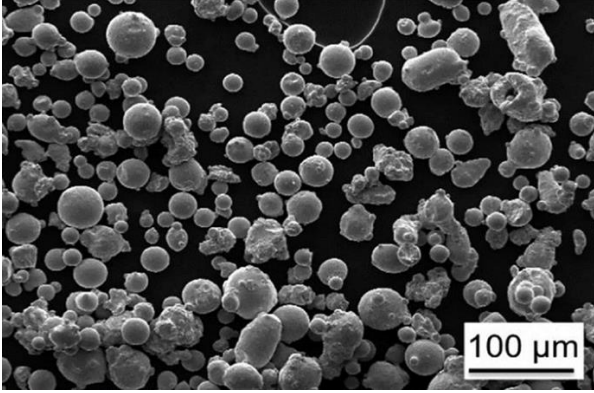


Figure 18. SEM micrograph and particle size distribution for commercial EOS IN 718 powder.

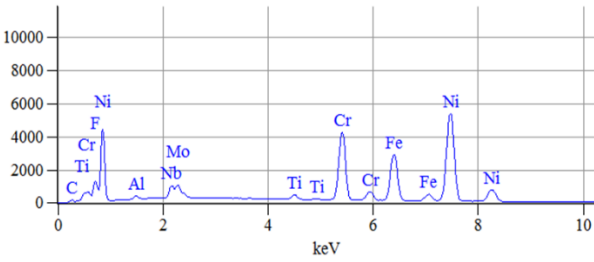
Figure 29 depicts the elemental analysis performed by EDS on the surface of fresh powder particles. According to expectations, Ni was the dominant element during evaluation, accounting for 52 % weight. When the composition of fresh IN718 powder and wrought IN718 sample was compared, the fresh powder study showed a 2% increase in chromium concentration. This enhances the effectiveness of the oxidation resistance of additively processed samples. [168]. On the other side, the iron content of fresh powder was 1% higher than that of wrought samples, which can have a negative effect.



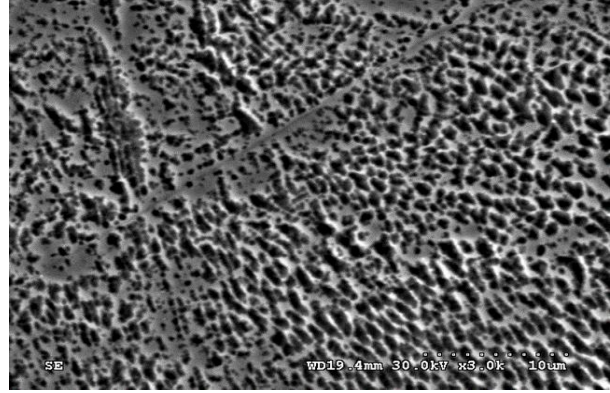
a)

Wt. %	C
<i>C</i>	1.33
<i>F</i>	1.00
<i>Al</i>	0.36
<i>Ti</i>	1.19
<i>Cr</i>	20.03
<i>Fe</i>	17.76
<i>Ni</i>	52.22
<i>Nb</i>	3.64
<i>Mo</i>	2.47

b)



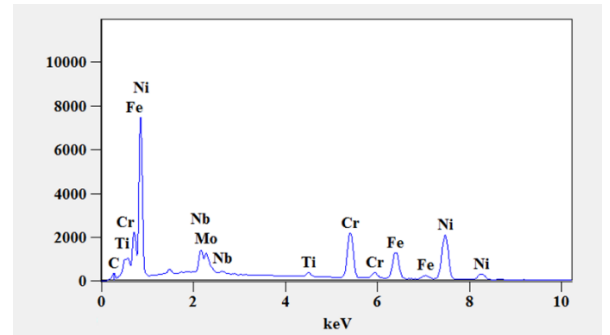
c)



d)

Wt. %	C
<i>C</i>	5.525
<i>Al</i>	21.885
<i>Ti</i>	1.555
<i>Cr</i>	21.885
<i>Fe</i>	17.021
<i>Ni</i>	40.651
<i>Nb</i>	7.917
<i>Mo</i>	5.444

e)

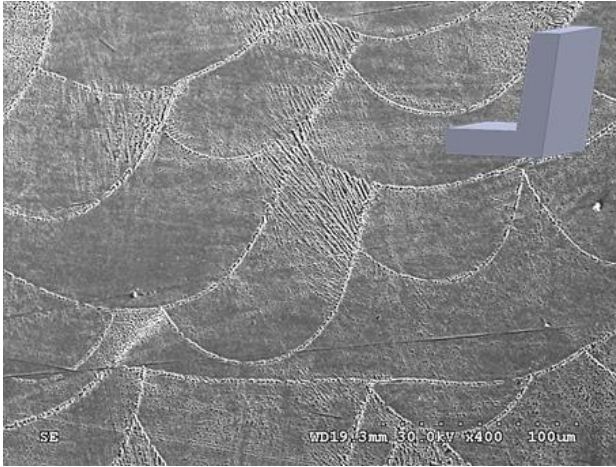


f)

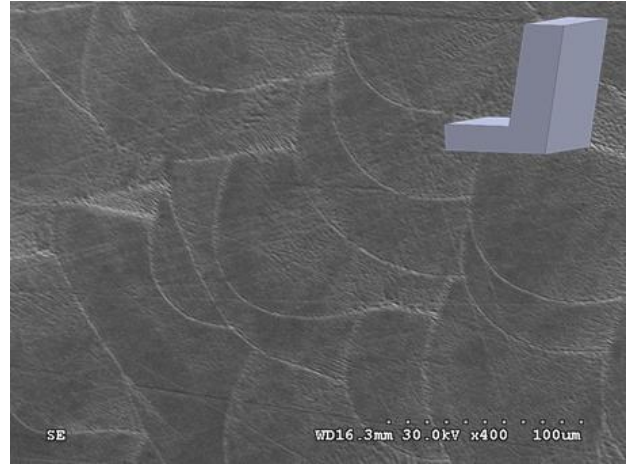
Figure 19. (a) SEM of fresh IN718 powder; (b) table describing percentage composition for each element in the fresh powder; (c) EDS compositions of IN718 fresh powder tested; (d) SEM of as fabricated sample; (e) table describing percentage composition for each element in as fabricated sample; (f) EDS compositions of as fabricated sample.

Then, in Figure 20, the SEM picture of the side surface of the main parts along the building path is presented. Due to the laser beam passes of each layer, the images show melt pools with a Gaussian form. As is being shown, different overhang thicknesses have an impact on the melt pool width in the side surface of fabricated pieces. The melt pool widths determined from each sample are listed in Table 5. The average melt pool width for overhang samples with varying thickness ranges from 98.25 μm to 128.27 μm and average melt pool depth ranges from 54.66 to 69.23 for samples A75T3 and A75T6 respectively. For the overhang samples fabricated with constant angle of 75 degrees and varying thickness from 3mm to 6mm, increasing trend in average melt pool size was observed as we can see in Table 4.

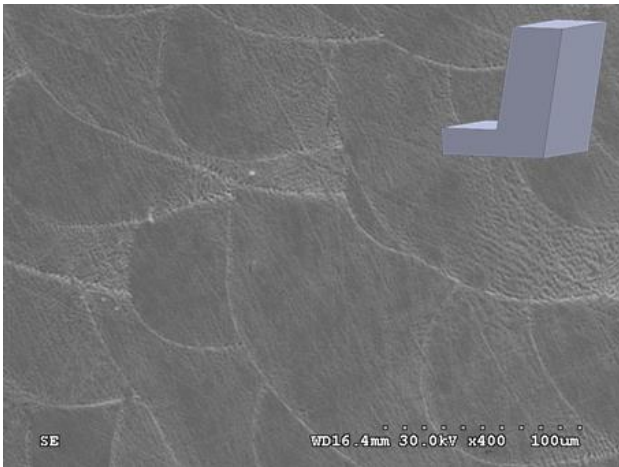
As thickness of overhang increases the surface area of fabricated layer also increases, in this case the heat dissipation rate increases which results in bigger melt pool compared to an overhang with lesser thickness, it can be concluded that a low thermal spread rate corresponds to a smaller melt pool [169-171]. Since the melt pool widths are constrained to smaller dimensions, the higher volumetric energy density resulting from the same energy being deposited increases grain formation, resulting in higher hardness in samples A75T3 and A75T6. For the samples fabricated with constant thickness and varying angle from 45, 60, 75, 90 degrees no significant relationship between variation in melt pool size and overhang angle was not found, But the decrease in melt pool width and depth was observed, the average melt pool width varied from 128.56 μm to 116.22 μm and the average melt pool depth varied from 54.66 μm to 65.96 μm . As per the results bigger melt pools was observed at 45-degree inclination and smaller melt pools were observed inclination 90 degree. This is because the surface area of the fabricated layer at lower inclination is bigger compared to the samples fabricated at higher inclination.



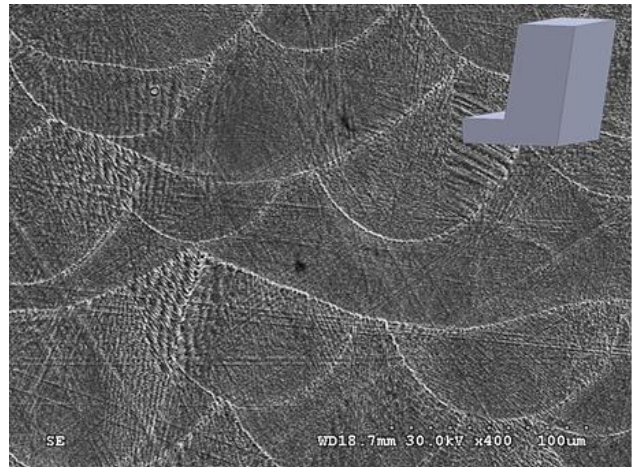
a)



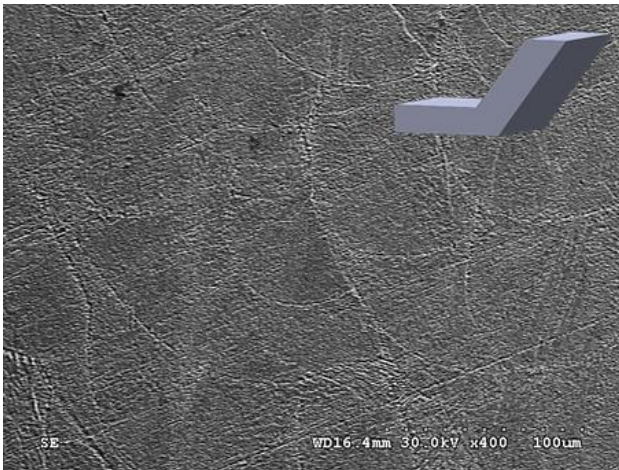
b)



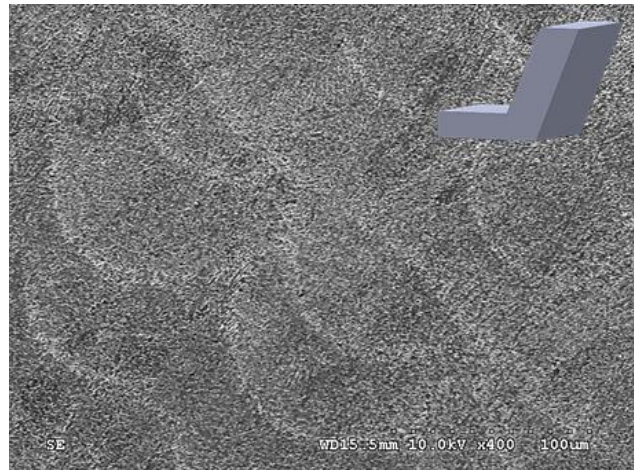
c)



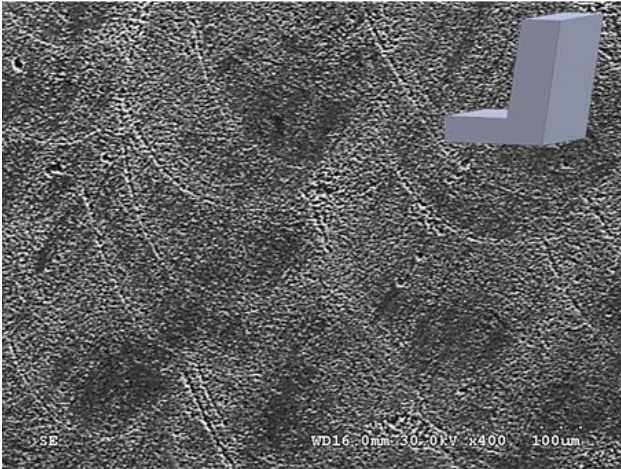
d)



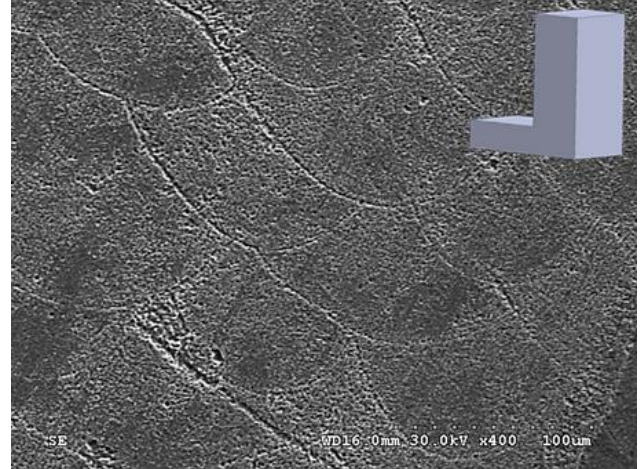
e)



f)






g)





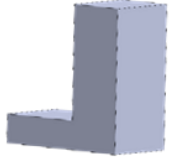


h)

Figure 20. SEM images of melt pool size for a) A75T3; b) A75T4; c) A75T5; d) A75T6; e) A45T4; f) A60T4; g) A75T4; h) A90T4.

Table 4. Effect of overhang parameters (Angle and Thickness) on the melt pool size and grain structure of as fabricated samples

Sample number	Symbol	Overhang structure	melt pool width (μm)	melt pool depth (μm)
1	A75T3		98.25	54.66
2	A75T4		117.79	60.05
3	A75T5		123.37	70.88

4	A75T6		128.27	69.23
5	A45T4		128.56	65.96
6	A60T4		118.13	61.03
7	A75T4		123.73	66.56
8	A90T4		116.22	66.152

4.2. Compositional analysis

Compositional analysis was performed using XRD on the fresh powder and fabricated parts as shown Figure 21. As it was expected, different phases for the fresh powder and all 8 overhang IN718

samples were found to be γ (Ni, Cr, Fe, C), γ' (Ni₃(Al,Ti)), γ'' (Ni₃Nb) and δ (C(Ni,Ti)). As shown, XRD peaks occur at the almost same angle in fabricated overhang samples at 2θ equal to 44°, 51°, 75°, and 90°, respectively.

The interpretation of XRD results reveals that the overhang structure has a direct effect on the fabricated main part. The γ , γ' and γ'' phases for fresh powder, and overhang sample are presented in Figure 21. As it was expected γ phase found to be the major phase in all the overhang samples, and the rest comprised mostly of γ' and γ'' phases. Although there are signs of δ phase in the supports, the quantity as compared to γ , γ' and γ'' phases is highly negligible and thus can be ignored. In comparison, the γ'' in sample was higher than other samples. This phase (γ'' (Ni₃Nb precipitate)) is associated with higher strength of fabricated part up to 650 °C [172]. Since the XRD findings for fresh powder and fabricated overhang show no discernible phase transition, we may conclude that fabricating Inconel 718 components using the SLM process has no impact on the phase changes.

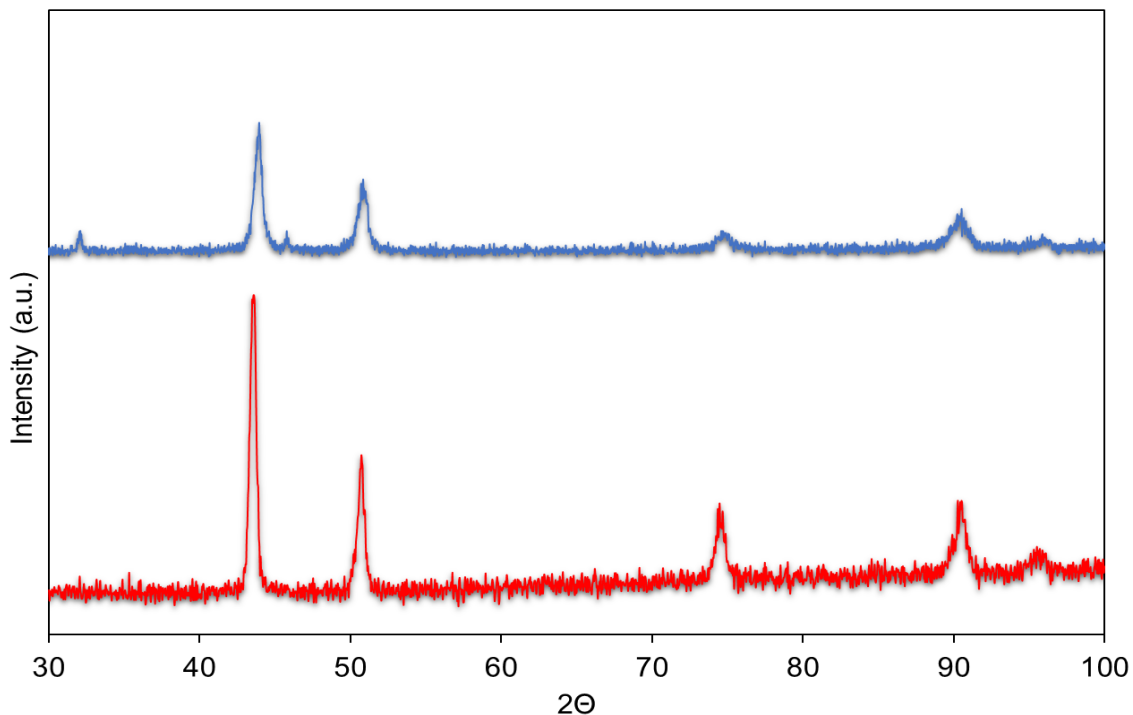


Figure 21. XRD image of fresh powder and overhang samples.

4.3. Hardness analysis

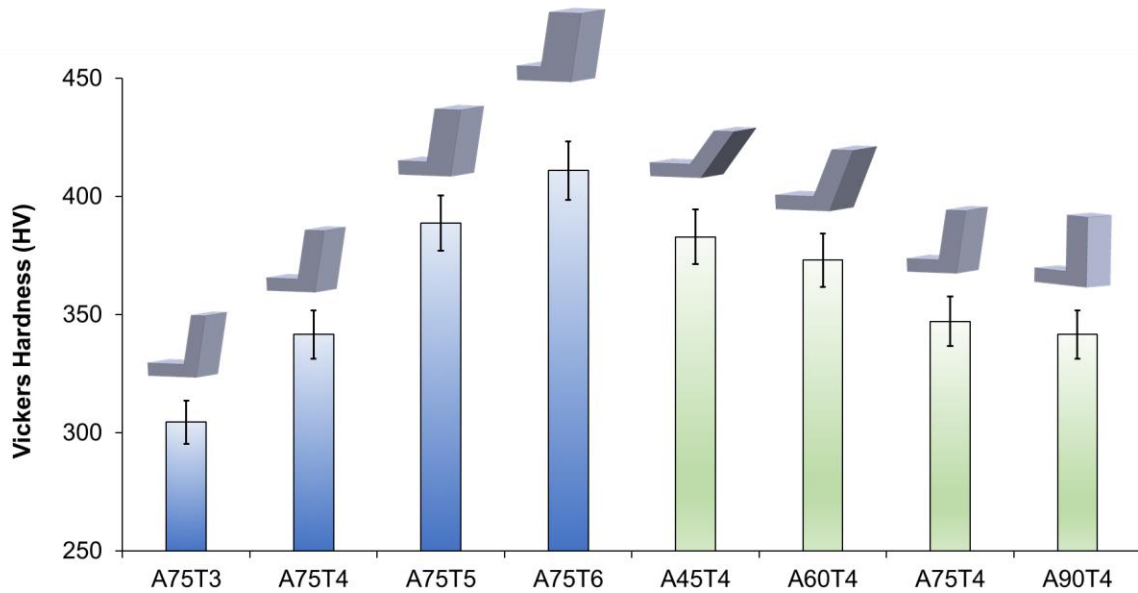


Figure 22. Vickers hardness results for all 8 overhang samples with varying angle and thickness.

Vickers hardness tests were conducted on each sample at the bottom of the overhang to determine the impact of thickness and angle on the as-built specimens. Two set of hardness data were analyzed, one for overhangs with constant inclination of 75 degree and having a varying thickness, which is in blue color and second set of hardness data for overhangs with constant thickness of 4mm and varying angle as shown in Figure 22. As the thickness increases, the hardness of a fabricated overhangs sample also increases. Vickers hardness was determined to be 304.48 HV, 341.62 HV, 388.79HV and 410.96HV for a sample A75T3, A75T4, A75T5 and A75T6 respectively. From the above hardness values, we were able to build a relationship between the effect of hardness over varying thickness of an overhang sample.

The reverse trend was absorbed in the hardness results for samples fabricated with constant thickness and varying angle. From the Figure 22 we can observe that as the inclination of a overhangs without supports increases the hardness decreases. Vickers harness was determined to be 382.90HV, 373.02HV, 347.15HV and 341.55HV for sample A45T4, A60T4, A75T4 and A90T4 respectively.

Hardness and energy density have been shown to have a strong relationship. The volume of the printed component available around the melt-pool expands as the overhang thickness is increased, raising the rate of heat conduction. Since energy density is inversely proportional to material volume, the energy density at the melt pool increases as the thickness of the overhang decreases with the same energy deposited at the melt pool area over all the overhang samples. The full melting of powder with less porosity, which is directly dependent on the energy density available at the melt pool area, determines the hardness of an as-printed sample [173].

Previous research has shown that grains appear to expand in the direction of the thermal gradient [169, 171]. The tensile strength of a component increases in the direction of grain growth, which is proportional to hardness [174]. It's worth noting that a material's thermal conductivity in powder form is lower than that of the printed element [86]. As a consequence, it's possible that the cooling rate is affected by the increased amount of printed sample. Faster heat transfer rates shorten the time it takes for grain structures to form, reducing the sample's weight.

Chapter 5. Conclusions and Future Works

5.1. Conclusion

In this study, different overhang geometries without support structures of Inconel 718 were fabricated in SLM. The study's motivation is to correlate the effects of different overhang geometry on the microstructure and mechanical properties of the Inconel 718 specimen. The effect different overhang structures with varying angle and thickness on the microstructure and mechanical properties was investigated systematically through SEM, EDS, XRD and Vickers hardness test, respectively. The following conclusions are shown below.

1. From the EDS results generated for both fresh powder and overhang sample shows that there are no recognizable changes in chemical combination between powder and sample.
2. XRD results showed that there is not change in phases between fresh Inconel718 powder and fabricate overhang sample, from the results the γ' , γ'' and δ phase peak occurs at almost same angle i.e., 2θ equal to 44° , 51° , 75° , and 90° for both powder as well as fabricated overhang samples.
3. The SEM micrographs show, the increase in melt pool size was observe as the overhang thickness varied from 3 mm to 6 mm with a constant inclination of 75 degree. But when the inclination of the overhang samples was increased from 45 degrees to 90 degrees with constant thickness of 4mm, the decrease in melt pool size was observed. This variation is due to the change in surface area of a fabricated layer associate with heat dissipation rate.
4. Vickers hardness analysis was used to investigate the impact of overhang thickness and angle on SLM fabricated IN718 samples. As the thickness of the overhang samples were increased with constant thickness the increase in hardness value was observed. From the results significant relationship has been formed between the thickness of the overhang and the hardness values.

5. As the angle of the overhangs increased with constant thickness, the hardness values showed a reversal pattern. The hardness results obtained for samples with varying angles was insufficient to draw comprehensive conclusions between the hardness value and the overhang samples with varying angles.
6. Since hardness values are affected by cooling rate and local energy density, a increase in hardness value was observed when the thickness of the fabricated overhang samples increased from 3mm to 6mm, and decrease in hardness value was observed when the angle of for a fabricated overhang sample were increased from 45 degree to 90 degree.

5.2. Future Work

Since the grain composition of AM parts varies from the support side to the top in the build course, changes in microstructure can be investigated. Due to the low quality of the SEM images used to observe the melt pool, a close correlation between microstructure changes and overhangs fabricated with differing angle and thickness could not be established. More research on overhang samples should be conducted using FESEM (Field emission scanning electron microscopy), which allows us to capture high resolution images of microstructure results. Furthermore, we can detect the microstructural changes as well as the precipitation caused by the change in overhang state by using TEM (Transmission Electron Microscopy).

Tensile and fatigue tests should be conducted on the overhang samples to build a more comprehensive conclusion between the decrease in hardness value as we increased the inclination of the overhang samples. If our investigation of hardness at different angles was right, it would aid in minimizing material use since the sample height will be low and will attain better mechanical properties when constructed with an inclination. For more precise results, samples can be manufactured with smaller increments of angle, such as 5-degree increments, and 1 degree increments in future fabrication.

Reference

- [1] Y. Huang, M.C. Leu, J. Mazumder, A. Donmez, Additive Manufacturing: Current State, Future Potential, Gaps and Needs, and Recommendations, *Journal of Manufacturing Science and Engineering* 137(1) (2015).
- [2] K.V. Wong, A. Hernandez, A Review of Additive Manufacturing, *ISRN Mechanical Engineering* 2012 (2012) 208760.
- [3] J. Jang, H.-G. Yi, D.-W. Cho, 3D Printed Tissue Models: Present and Future, *ACS Biomaterials Science & Engineering* 2(10) (2016) 1722-1731.
- [4] M. Singh, S. Jonnalagadda, Advances in bioprinting using additive manufacturing, *European Journal of Pharmaceutical Sciences* 143 (2020) 105167.
- [5] A. Uriondo, M. Esperon-Miguez, S. Perinpanayagam, The present and future of additive manufacturing in the aerospace sector: A review of important aspects, *229(11)* (2015) 2132-2147.
- [6] K. Biswas, J. Rose, L. Eikevik, M. Guerguis, P. Enquist, B. Lee, L. Love, J. Green, R. Jackson, Additive Manufacturing Integrated Energy—Enabling Innovative Solutions for Buildings of the Future, *Journal of Solar Energy Engineering* 139(1) (2016).
- [7] globalsources. <https://www.globalsources.com/gsol/I/Mascara/a/9000000146361.htm>.
- [8] A. Bevan, 3-D printed sets and props: How designers integrate digital technologies, *24(6)* (2018) 554-567.
- [9] A. Bhargav, V. Sanjairaj, V. Rosa, L.W. Feng, J. Fuh YH, Applications of additive manufacturing in dentistry: A review, *106(5)* (2018) 2058-2064.
- [10] Y.-a. Jin, J. Plott, R. Chen, J. Wensman, A. Shih, Additive Manufacturing of Custom Orthoses and Prostheses – A Review, *Procedia CIRP* 36 (2015) 199-204.
- [11] T.m.i. sculpteo. <https://www.sculpteo.com/blog/wp-content/uploads/2017/01/titanium-medical-implants-sculpteo.jpg>.

- [12] U.E. Klotz, D. Tiberto, F. Held, Optimization of 18-karat yellow gold alloys for the additive manufacturing of jewelry and watch parts, *Gold Bulletin* 50(2) (2017) 111-121.
- [13] B.H.a.G. Wilson, 3D/additive printing manufacturing: A BRIEF HISTORY AND PURCHASING GUIDE, *Technology and Engineering Teacher* vol. 75 (2016).
- [14] I.a.R. Gibson, David and Stucker, Brent and Khorasani, Mahyar, *Additive manufacturing technologies*, Springer2014.
- [15] S.H.a.P. Khajavi, Jouni and Holmstr, Additive manufacturing in the spare parts supply chain, *Computers in industry* 65 (2014) 50--63.
- [16] J.-P.a.L. Kruth, Ming-Chuan and Nakagawa, Terunaga, Progress in additive manufacturing and rapid prototyping, *Cirp Annals* 47 (1998) 525--540.
- [17] G. Additive. <https://www.ge.com/additive/additive-manufacturing/industries/aviation-aerospace>.
- [18] C. Deckard, Patent US 4863538-A, Method and apparatus for producing parts by selective sintering (1986).
- [19] A. Lou, C. Grosvenor, Selective laser sintering, birth of an industry, Department of Mechanical Engineering, University of Texas, Austin, TX (2012).
- [20] S.F. Kabir, K. Mathur, A.-F.M. Seyam, A critical review on 3D printed continuous fiber-reinforced composites: History, mechanism, materials and properties, *Composite Structures* 232 (2020) 111476.
- [21] C.R. Deckard, Method and apparatus for producing parts by selective sintering, Google Patents, 1989.
- [22] EOS GmbH, History, April 16. <https://www.eos.info/30-years-of-EOS>.
- [23] W. Harun, N. Manam, M. Kamariah, S. Sharif, A. Zulkifly, I. Ahmad, H. Miura, A review of powdered additive manufacturing techniques for Ti-6Al-4V biomedical applications, *Powder Technology* 331 (2018) 74-97.
- [24] P. EBM, LENS, and Polyjet were nonexistent Arcam-AB., Arcam History., (April 16).
- [25] T. Wohlers, T. Gornet, History of additive manufacturing, *Wohlers report* 24(2014) (2014) 118.
- [26] J.-P. Kruth, Material in excess manufacturing by rapid prototyping techniques, *CIRP annals* 40(2) (1991) 603-614.

- [27] D.L. Bourell, Rapid prototyping journal, EMERALD GROUP PUBLISHING LIMITED 60/62 TOLLER LANE, BRADFORD BD8 9BY, W ..., 2007.
- [28] E. Sells, S. Bailard, Z. Smith, A. Bowyer, V. Olliver, RepRap: the replicating rapid prototyper: maximizing customizability by breeding the means of production, Handbook of Research in Mass Customization and Personalization: (In 2 Volumes), World Scientific 2010, pp. 568-580.
- [29] O. Es-Said, J. Foyos, R. Noorani, M. Mendelson, R. Marloth, B. Pregger, Effect of layer orientation on mechanical properties of rapid prototyped samples, Materials and Manufacturing Processes 15(1) (2000) 107-122.
- [30] J. Gardan, Additive manufacturing technologies: state of the art and trends, International Journal of Production Research 54(10) (2016) 3118-3132.
- [31] K.V. Wong, A. Hernandez, A review of additive manufacturing, International scholarly research notices 2012 (2012).
- [32] Q. Jia, D. Gu, Selective laser melting additive manufactured Inconel 718 superalloy parts: high-temperature oxidation property and its mechanisms, Optics & Laser Technology 62 (2014) 161-171.
- [33] N. Raghavan, R. Dehoff, S. Pannala, S. Simunovic, M. Kirka, J. Turner, N. Carlson, S.S. Babu, Numerical modeling of heat-transfer and the influence of process parameters on tailoring the grain morphology of IN718 in electron beam additive manufacturing, Acta Materialia 112 (2016) 303-314.
- [34] W. Tillmann, C. Schaak, J. Nellesen, M. Schaper, M. Aydinöz, K.-P. Hoyer, Hot isostatic pressing of IN718 components manufactured by selective laser melting, Additive Manufacturing 13 (2017) 93-102.
- [35] C. Körner, H. Helmer, A. Bauereiß, R.F. Singer, Tailoring the grain structure of IN718 during selective electron beam melting, MATEC Web of Conferences, EDP Sciences, 2014, p. 08001.
- [36] A. Hinojos, J. Mireles, A. Reichardt, P. Frigola, P. Hosemann, L.E. Murr, R.B. Wicker, Joining of Inconel 718 and 316 Stainless Steel using electron beam melting additive manufacturing technology, Materials & Design 94 (2016) 17-27.
- [37] D.M. Lambert, IN718 additive manufacturing properties and influences, (2015).

- [38] Y. Zhang, X. Cao, P. Wanjara, Microstructure and hardness of fiber laser deposited Inconel 718 using filler wire, *The International Journal of Advanced Manufacturing Technology* 69(9-12) (2013) 2569-2581.
- [39] V. Popovich, E. Borisov, A. Popovich, V.S. Sufiiarov, D. Masaylo, L. Alzina, Functionally graded Inconel 718 processed by additive manufacturing: Crystallographic texture, anisotropy of microstructure and mechanical properties, *Materials & Design* 114 (2017) 441-449.
- [40] Y. Tian, D. McAllister, H. Colijn, M. Mills, D. Farson, M. Nordin, S. Babu, Rationalization of microstructure heterogeneity in INCONEL 718 builds made by the direct laser additive manufacturing process, *Metallurgical and Materials Transactions A* 45(10) (2014) 4470-4483.
- [41] K. Moussaoui, W. Rubio, M. Mousseigne, T. Sultan, F. Rezai, Effects of Selective Laser Melting additive manufacturing parameters of Inconel 718 on porosity, microstructure and mechanical properties, *Materials Science and Engineering: A* 735 (2018) 182-190.
- [42] I. Yadroitsev, I. Smurov, Selective laser melting technology: from the single laser melted track stability to 3D parts of complex shape, *Physics Procedia* 5 (2010) 551-560.
- [43] S. Huang, F. You, H. Peng, W. Luo, Y. Feng, S. Lv, L. Sun, C. Yan, Influence of surface on spectroscopic properties of rare earth ions in nanocrystals, *Journal of Rare Earth* 25(4) (2007) 396-401.
- [44] M. Elahinia, N.S. Moghaddam, M.T. Andani, A. Amerinatanzi, B.A. Bimber, R.F. Hamilton, Fabrication of NiTi through additive manufacturing: A review, *Progress in Materials Science* 83 (2016) 630-663.
- [45] M. Elahinia, N.S. Moghaddam, M.T. Andani, R. Rahmanian, J. Walker, M. Miller, D. Dean, Site-specific material properties and the additive manufacturing of nitinol musculoskeletal implants, *Tissue Engineering Part A*, MARY ANN LIEBERT, INC 140 HUGUENOT STREET, 3RD FL, NEW ROCHELLE, NY 10801 USA, 2014, pp. S120-S121.
- [46] A. Amerinatanzi, H. Zamanian, N. Shayesteh Moghaddam, A. Jahadakbar, M. Elahinia, Application of the superelastic NiTi spring in ankle foot orthosis (AFO) to create normal ankle joint behavior, *Bioengineering* 4(4) (2017) 95.

- [47] N. Shayesteh Moghaddam, A. Jahadakbar, A. Amerinatanzi, R. Skoracki, M. Miller, D. Dean, M. Elahinia, Fixation release and the bone bandaid: A new bone fixation device paradigm, *Bioengineering* 4(1) (2017) 5.
- [48] B. Zhang, H. Liao, C. Coddet, Microstructure evolution and density behavior of CP Ti parts elaborated by self-developed vacuum selective laser melting system, *Applied surface science* 279 (2013) 310-316.
- [49] L. Dong, H. Wang, Microstructure and corrosion properties of laser-melted deposited Ti₂Ni₃Si/NiTi intermetallic alloy, *Journal of Alloys and Compounds* 465(1-2) (2008) 83-89.
- [50] B. Zhang, H. Liao, C. Coddet, Selective laser melting commercially pure Ti under vacuum, *Vacuum* 95 (2013) 25-29.
- [51] S. Saedi, S.E. Saghaian, A. Jahadakbar, N.S. Moghaddam, M.T. Andani, S.M. Saghaian, Y.C. Lu, M. Elahinia, H.E. Karaca, Shape memory response of porous NiTi shape memory alloys fabricated by selective laser melting, *Journal of Materials Science: Materials in Medicine* 29(4) (2018) 40.
- [52] A. Ahmadi, N. Shayesteh Moghaddam, M. Elahinia, H.E. Karaca, R. Mirzaeifar, Finite element modeling of selective laser melting 316l stainless steel parts for evaluating the mechanical properties, *International Manufacturing Science and Engineering Conference*, American Society of Mechanical Engineers, 2016, p. V002T01A003.
- [53] N.S. Moghaddam, A. Jahadakbar, M. Elahinia, D. Dean, M. Miller, The effect of adding dental implants to the reconstructed mandible comparing the effect of using Ti-6Al-4V and NiTi hardware, *Tissue Engineering Part A*, MARY ANN LIEBERT, INC 140 HUGUENOT STREET, 3RD FL, NEW ROCHELLE, NY 10801 USA, 2015, pp. S398-S398.
- [54] S. Thakare, B.B. Ravichander, N. Swails, N.S. Moghaddam, A. Amerinatanzi, The effect of support structure geometry on surface topography of selectively laser melted parts, *Behavior and Mechanics of Multifunctional Materials IX*, International Society for Optics and Photonics, 2020, p. 113771D.
- [55] H. Ibrahim, A. Jahadakbar, A. Dehghan, N.S. Moghaddam, A. Amerinatanzi, M. Elahinia, In vitro corrosion assessment of additively manufactured porous NiTi structures for bone fixation applications, *Metals* 8(3) (2018) 164.

- [56] A. Jahadakbar, N. Shayesteh Moghaddam, A. Amerinatanzi, D. Dean, H.E. Karaca, M. Elahinia, Finite element simulation and additive manufacturing of stiffness-matched niti fixation hardware for mandibular reconstruction surgery, *Bioengineering* 3(4) (2016) 36.
- [57] A. Dehghanghadikolaei, H. Ibrahim, A. Amerinatanzi, M. Hashemi, N.S. Moghaddam, M. Elahinia, Improving corrosion resistance of additively manufactured nickel–titanium biomedical devices by micro-arc oxidation process, *Journal of materials science* 54(9) (2019) 7333-7355.
- [58] N.S. Moghaddam, S. Saedi, A. Amerinatanzi, A. Hinojos, A. Ramazani, J. Kundin, M.J. Mills, H. Karaca, M. Elahinia, Achieving superelasticity in additively manufactured NiTi in compression without post-process heat treatment, *Scientific reports* 9(1) (2019) 1-11.
- [59] Q. Jia, D. Gu, Selective laser melting additive manufacturing of Inconel 718 superalloy parts: Densification, microstructure and properties, *Journal of Alloys and Compounds* 585 (2014) 713-721.
- [60] K. Shahzad, J. Deckers, Z. Zhang, J.-P. Kruth, J. Vleugels, Additive manufacturing of zirconia parts by indirect selective laser sintering, *Journal of the European Ceramic Society* 34(1) (2014) 81-89.
- [61] N.S. Moghaddam, A. Jahadakbar, A. Amerinatanzi, M. Elahinia, Recent advances in laser-based additive manufacturing, *Laser-Based Additive Manufacturing of Metal Parts*, CRC Press 2017, pp. 1-24.
- [62] C.K. Chua, K.F. Leong, C.S. Lim, *Rapid prototyping: principles and applications (with companion CD-ROM)*, World Scientific Publishing Company 2010.
- [63] J.-P. Kruth, G. Levy, F. Klocke, T. Childs, Consolidation phenomena in laser and powder-bed based layered manufacturing, *CIRP annals* 56(2) (2007) 730-759.
- [64] J. Delgado, J. Ciurana, C.A. Rodríguez, Influence of process parameters on part quality and mechanical properties for DMLS and SLM with iron-based materials, *The International Journal of Advanced Manufacturing Technology* 60(5-8) (2012) 601-610.
- [65] D.a.B. Atkinson, Chris and Cobb, Richard, *Rapid prototyping and tooling: a practical guide*, (1997).
- [66] P.a.E. Regenfuss, Robby and Exner, Horst, Laser micro sintering--a versatile instrument for the generation of microparts, *Laser Technik Journal* 4 (2007) 26--31.

- [67] P. Regenfuss, R. Ebert, H. Exner, Laser micro sintering—a versatile instrument for the generation of microparts, *Laser Technik Journal* 4(1) (2007) 26-31.
- [68] P. Regenfuss, L. Hartwig, S. Klotzer, R. Ebert, H. Exner, Microparts by a novel modification of selective laser sintering, *TECHNICAL PAPERS-SOCIETY OF MANUFACTURING ENGINEERS-ALL SERIES-* (2004).
- [69] E. Aliakbari, H. Baseri, Optimization of machining parameters in rotary EDM process by using the Taguchi method, *The International Journal of Advanced Manufacturing Technology* 62(9-12) (2012) 1041-1053.
- [70] R. Udriou, POWDER BED ADDITIVE MANUFACTURING SYSTEMS AND ITS APPLICATIONS, *Academic journal of manufacturing engineering* 10(4) (2012).
- [71] V. Petrovic, J. Vicente Haro Gonzalez, O. Jordá Ferrando, J. Delgado Gordillo, J. Ramón Blasco Puchades, L. Portolés Griñan, Additive layered manufacturing: sectors of industrial application shown through case studies, *International Journal of Production Research* 49(4) (2011) 1061-1079.
- [72] S. Saedi, A.S. Turabi, M.T. Andani, N.S. Moghaddam, M. Elahinia, H.E. Karaca, Texture, aging, and superelasticity of selective laser melting fabricated Ni-rich NiTi alloys, *Materials Science and Engineering: A* 686 (2017) 1-10.
- [73] R. Rahmanian, N.S. Moghaddam, C. Haberland, D. Dean, M. Miller, M. Elahinia, Load bearing and stiffness tailored niti implants produced by additive manufacturing: a simulation study, *Behavior and Mechanics of Multifunctional Materials and Composites 2014*, International Society for Optics and Photonics, 2014, p. 905814.
- [74] N.S. Moghaddam, M. Elahinia, M. Miller, D. Dean, Enhancement of bone implants by substituting nitinol for titanium (Ti-6Al-4V): A modeling comparison, *Smart Materials, Adaptive Structures and Intelligent Systems*, American Society of Mechanical Engineers, 2014, p. V001T03A031.
- [75] H.D. Dean, M.H. Elahinia, C. Haberland, M.J. Miller, A. Sutradhar, N.S. Moghaddam, J.M. Walker, R. Skoracki, Methods, devices, and manufacture of the devices for musculoskeletal reconstructive surgery, *Google Patents*, 2017.

- [76] A. Hadi, M. Qasemi, M. Elahinia, N. Moghaddam, Modeling and experiment of a flexible module actuated by shape memory alloy wire, Smart Materials, Adaptive Structures and Intelligent Systems, American Society of Mechanical Engineers, 2014, p. V001T03A035.
- [77] B. Raad, N.S. Moghaddam, M. Elahinia, A numerical simulation of the effect of using porous superelastic Nitinol and stiff Titanium fixation hardware on the bone remodeling, Nanosensors, Biosensors, and Info-Tech Sensors and Systems 2016, International Society for Optics and Photonics, 2016, p. 98021T.
- [78] A.A. Bharath Bhushan Ravichander, Narges Shayesteh Moghaddam, Study on the Effect of Powder-Bed Fusion Process Parameters on the Quality of as-Built IN718 Parts Using Response Surface Methodology, Metals 10 (2020) 1180.
- [79] B.F. Bharath Bhushan Ravichander, Nahid Swails, Amirhesam Amerinatanzi, Narges Shayesteh Moghaddam, Analysis of the deviation in properties of selective laser melted samples fabricated by varying process parameters, Behavior and Mechanics of Multifunctional Materials IX, 2020, p. 113771A.
- [80] C.F. Bharath Bhushan Ravichander, Amirhesam Amerinatanzi, Narges Shayesteh Moghaddam, A framework for the optimization of powder-bed fusion process, Behavior and Mechanics of Multifunctional Materials XV, International Society for Optics and Photonics, 2021, p. 115890N.
- [81] I. Yadroitsev, P. Bertrand, I. Smurov, Parametric analysis of the selective laser melting process, Applied surface science 253(19) (2007) 8064-8069.
- [82] Z.Y. Bharath Bhushan Ravichander, Chen Kan, Narges Shayesteh Moghaddam, Amirhesam Amerinatanzi, Development of ANN model for surface roughness prediction of parts produced by varying fabrication parameters, Behavior and Mechanics of Multifunctional Materials XV, International Society for Optics and Photonics, 2021, p. 115890M.
- [83] B.B. Ravichander, CORRELATION AND EFFECT OF PROCESS PARAMETERS ON THE PROPERTIES OF INCONEL 718 PARTS FABRICATED BY SELECTIVE LASER MELTING USING RESPONSE SURFACE METHOD, 2020.

- [84] M. Elahinia, N.S. Moghaddam, A. Amerinatanzi, S. Saedi, G.P. Toker, H. Karaca, G.S. Bigelow, O. Benafan, Additive manufacturing of NiTiHf high temperature shape memory alloy, *Scripta Materialia* 145 (2018) 90-94.
- [85] A. Ahmadi, R. Mirzaeifar, N.S. Moghaddam, A.S. Turabi, H.E. Karaca, M. Elahinia, Effect of manufacturing parameters on mechanical properties of 316L stainless steel parts fabricated by selective laser melting: A computational framework, *Materials & Design* 112 (2016) 328-338.
- [86] C. Ma, M.T. Andani, H. Qin, N.S. Moghaddam, H. Ibrahim, A. Jahadakbar, A. Amerinatanzi, Z. Ren, H. Zhang, G.L. Doll, Improving surface finish and wear resistance of additive manufactured nickel-titanium by ultrasonic nano-crystal surface modification, *Journal of Materials Processing Technology* 249 (2017) 433-440.
- [87] S.N. Esfahani, M.T. Andani, N.S. Moghaddam, R. Mirzaeifar, M. Elahinia, Independent tuning of stiffness and toughness of additively manufactured titanium-polymer composites: Simulation, fabrication, and experimental studies, *Journal of Materials Processing Technology* 238 (2016) 22-29.
- [88] N.S. Moghaddam, A. Jahadakbar, A. Amerinatanzi, M. Elahinia, M. Miller, D. Dean, Metallic fixation of mandibular segmental defects: Graft immobilization and orofacial functional maintenance, *Plastic and Reconstructive Surgery Global Open* 4(9) (2016).
- [89] N.S. Moghaddam, M.T. Andani, A. Amerinatanzi, C. Haberland, S. Huff, M. Miller, M. Elahinia, D. Dean, Metals for bone implants: Safety, design, and efficacy, *Biomanufacturing Reviews* 1(1) (2016) 1-16.
- [90] S. Saedi, N.S. Moghaddam, A. Amerinatanzi, M. Elahinia, H.E. Karaca, On the effects of selective laser melting process parameters on microstructure and thermomechanical response of Ni-rich NiTi, *Acta Materialia* 144 (2018) 552-560.
- [91] N.S. Moghaddam, R. Skoracki, M. Miller, M. Elahinia, D. Dean, Three dimensional printing of stiffness-tuned, nitinol skeletal fixation hardware with an example of mandibular segmental defect repair, *Procedia CIRP* 49 (2016) 45-50.
- [92] N. Shayesteh Moghaddam, Toward patient specific long lasting metallic implants for mandibular segmental defects, University of Toledo, 2015.

- [93] B.B.R. Behzad Farhang, Federico Venturi, Amirhesam Amerinatanzi, Narges Shayesteh Moghaddam, Study on variations of microstructure and metallurgical properties in various heat-affected zones of SLM fabricated Nickel–Titanium alloy, *Materials Science and Engineering: A* 774 (2020) 138919.
- [94] H.K.T. Kiriti Mamidi, Bharath Bhushan Ravichander, Behzad Farhang, Narges Shayesteh Moghaddam, Amirhesam Amerinatanzi, Study on the influence of post-processing parameters over microstructure and metallurgical properties of NiTi alloy, *Behavior and Mechanics of Multifunctional Materials IX*, International Society for Optics and Photonics, 2020, p. 113770V.
- [95] A.A. Bharath Bhushan Ravichander, Narges Shayesteh Moghaddam, Toward mitigating microcracks using nanopowders in laser powder bed fusion, *Behavior and Mechanics of Multifunctional Materials XV*, International Society for Optics and Photonics, 2021, p. 115890P.
- [96] H. Gu, H. Gong, D. Pal, K. Rafi, T. Starr, B. Stucker, Influences of energy density on porosity and microstructure of selective laser melted 17-4PH stainless steel, 2013 Solid Freeform Fabrication Symposium, 2013.
- [97] Z. Hu, H. Zhu, H. Zhang, X. Zeng, Experimental investigation on selective laser melting of 17-4PH stainless steel, *Optics & Laser Technology* 87 (2017) 17-25.
- [98] H. Irrinki, M. Dexter, B. Barmore, R. Enneti, S. Pasebani, S. Badwe, J. Stitzel, R. Malhotra, S.V. Atre, Effects of powder attributes and laser powder bed fusion (L-PBF) process conditions on the densification and mechanical properties of 17-4 PH stainless steel, *Jom* 68(3) (2016) 860-868.
- [99] H. Attar, K.G. Prashanth, L.-C. Zhang, M. Calin, I.V. Okulov, S. Scudino, C. Yang, J. Eckert, Effect of powder particle shape on the properties of in situ Ti–TiB composite materials produced by selective laser melting, *Journal of Materials Science & Technology* 31(10) (2015) 1001-1005.
- [100] S. Kumar, 10.05 Selective Laser Sintering/Melting In *Comprehensive Materials Processing*; Hashmi, S., Ed, Elsevier: Amsterdam, 2014.
- [101] B.X. Cao, M. Bae, H. Sohn, J. Choi, Y. Kim, J.-o. Kim, J. Noh, Design and performance of a focus-detection system for use in laser micromachining, *Micromachines* 7(1) (2016) 2.

- [102] P. Hanzl, M. Zetek, T. Bakša, T. Kroupa, The influence of processing parameters on the mechanical properties of SLM parts, *Procedia Engineering* 100(1) (2015) 1405-1413.
- [103] M. Rombouts, J.-P. Kruth, L. Froyen, P. Mercelis, Fundamentals of selective laser melting of alloyed steel powders, *CIRP annals* 55(1) (2006) 187-192.
- [104] Y. Yang, H.T. Loh, J. Fuh, Y. Wang, Equidistant path generation for improving scanning efficiency in layered manufacturing, *Rapid Prototyping Journal* (2002).
- [105] Y. Shi, W. Zhang, Y. Cheng, S. Huang, Compound scan mode developed from subarea and contour scan mode for selective laser sintering, *International Journal of Machine Tools and Manufacture* 47(6) (2007) 873-883.
- [106] K.M. Vignesh RK Rajendran, Bharath Ravichander, Behzad Farhang, Amirhesam Amerinatanzi, Narges Shayesteh Moghaddam, Determination of residual stress for Inconel 718 samples fabricated through different scanning strategies in selective laser melting, *Behavior and Mechanics of Multifunctional Materials IX*, International Society for Optics and Photonics, 2020, p. 1137719.
- [107] G. Fernlund, A. Poursartip, G. Twigg, C. Albert, Residual stress, spring-in and warpage in autoclaved composite parts, *TECHNICAL PAPERS-SOCIETY OF MANUFACTURING ENGINEERS-ALL SERIES-* (2003).
- [108] R.B.B.a.S. Hanumantha Manjunath, Manya and Swails, Nahid and Amerinatanzi, Amirhesam, Spatial microstructural analysis for selective laser melted components, *Behavior and Mechanics of Multifunctional Materials XV* 11589 (2021) 115890L.
- [109] L.C. Zhang, H. Attar, Selective laser melting of titanium alloys and titanium matrix composites for biomedical applications: a review, *Advanced Engineering Materials* 18(4) (2016) 463-475.
- [110] S. Ashley, Rapid prototyping systems, *Mechanical Engineering* 113(4) (1991) 34.
- [111] R.I. Campbell, H. Jee, Y.S. Kim, Adding product value through additive manufacturing, *DS 75-4: Proceedings of the 19th International Conference on Engineering Design (ICED13), Design for Harmonies, Vol. 4: Product, Service and Systems Design, Seoul, Korea, 19-22.08. 2013, 2013.*

- [112] M. Ruffo, C. Tuck, R. Hague, Make or buy analysis for rapid manufacturing, *Rapid Prototyping Journal* (2007).
- [113] M.K. Thompson, G. Moroni, T. Vaneker, G. Fadel, R.I. Campbell, I. Gibson, A. Bernard, J. Schulz, P. Graf, B. Ahuja, Design for Additive Manufacturing: Trends, opportunities, considerations, and constraints, *CIRP annals* 65(2) (2016) 737-760.
- [114] B.P. Conner, G.P. Manogharan, A.N. Martof, L.M. Rodomsky, C.M. Rodomsky, D.C. Jordan, J.W. Limperos, Making sense of 3-D printing: Creating a map of additive manufacturing products and services, *Additive Manufacturing* 1 (2014) 64-76.
- [115] C.K. Chua, S.M. Chou, S.C. Lin, K.H. Eu, K.F. Lew, Rapid prototyping assisted surgery planning, *The International Journal of Advanced Manufacturing Technology* 14(9) (1998) 624-630.
- [116] R. Noorani, *Rapid prototyping: principles and applications*, John Wiley & Sons Incorporated 2006.
- [117] J. Flowers, M. Moniz, Rapid prototyping in technology education: rapid prototyping, while costly, can afford students a unique opportunity to bring their ideas to reality, *The Technology Teacher* 62(3) (2002) 7-12.
- [118] N. Guo, M.C. Leu, Additive manufacturing: technology, applications and research needs, *Frontiers of Mechanical Engineering* 8(3) (2013) 215-243.
- [119] D.L. Bourell, M.C. Leu, D.W. Rosen, Roadmap for additive manufacturing: identifying the future of freeform processing, *The University of Texas at Austin, Austin, TX* (2009) 11-15.
- [120] I. Campbell, D. Bourell, I. Gibson, Additive manufacturing: rapid prototyping comes of age, *Rapid prototyping journal* (2012).
- [121] g. bracket.
- [122] w.f.D.p. heart. <https://freearticle69.com/2020/12/07/world-first-3d-heart/>.
- [123] D.-p.o.b.n.l.i. bioengineering.
- [124] A. Lingenfelter, Welding of Inconel alloy 718: A historical overview, *Superalloy 718* (1989) 673-683.
- [125] S. Metals, Inconel alloy 718, Publication Number SMC-045. Special Metals Corporation (2007).

- [126] M.a.S. Lewandowski, V and Wilcox, RC and Matlock, CA and Overfelt, RA, High temperature deformation of Inconel 718 castings, *Superalloys 718* (1994) 625--706.
- [127] Z.a.R. Wang, Kamlakar P and Fan, J and Lei, S and Shin, YC and Petrescu, G, Hybrid machining of Inconel 718, *International Journal of Machine Tools and Manufacture* 43 (2003) 1391--1396.
- [128] S.a.R. Srivathsan, Bharath B and Moghaddam, Narges Shayesteh and Swails, Nahid and Amerinatanzi, Amirhesam, Investigation of the strength of different porous lattice structures manufactured using selective laser melting, 11377 (2020) 113771B.
- [129] G. Çam, M. Koçak, Progress in joining of advanced materials, *International Materials Reviews* 43(1) (1998) 1-44.
- [130] F. Liu, X. Lin, C. Huang, M. Song, G. Yang, J. Chen, W. Huang, The effect of laser scanning path on microstructures and mechanical properties of laser solid formed nickel-base superalloy Inconel 718, *Journal of Alloys and Compounds* 509(13) (2011) 4505-4509.
- [131] S.-H. Chang, In situ TEM observation of γ' , γ'' and δ precipitations on Inconel 718 superalloy through HIP treatment, *Journal of alloys and compounds* 486(1-2) (2009) 716-721.
- [132] MegaMex, Inconer718 Properties.
- [133] B. Kuriachen, J. Mathew, MODELING AND MULTI-RESPONSE PREDICTION OF MICRO EDM DRILLING ON INCONEL 718, All india manufacturing technology, design and research conference, 2014.
- [134] I.R.B. suppliers. <https://www.stindia.com/uns-n07718-inconel-alloy-718-round-bar-supplier.html>.
- [135] w.c.o.a.A.W. engine.
- [136] L. Zheng, G. Schmitz, Y. Meng, R. Chellali, R. Schlesiger, Mechanism of intermediate temperature embrittlement of Ni and Ni-based superalloys, *Critical Reviews in Solid State and Materials Sciences* 37(3) (2012) 181-214.
- [137] C.-M. Kuo, Y.-T. Yang, H.-Y. Bor, C.-N. Wei, C.-C. Tai, Aging effects on the microstructure and creep behavior of Inconel 718 superalloy, *Materials Science and Engineering: A* 510 (2009) 289-294.

- [138] Q.-l. Zhang, J.-h. Yao, J. Mazumder, Laser direct metal deposition technology and microstructure and composition segregation of Inconel 718 superalloy, *Journal of Iron and Steel Research, International* 18(4) (2011) 73-78.
- [139] B. Izquierdo, S. Plaza, J. Sánchez, I. Pombo, N. Ortega, Numerical prediction of heat affected layer in the EDM of aeronautical alloys, *Applied Surface Science* 259 (2012) 780-790.
- [140] L. Zheng, Z. Maicang, D. Jianxin, Hot corrosion behavior of powder metallurgy Rene95 nickel-based superalloy in molten NaCl–Na₂SO₄ salts, *Materials & Design* 32(4) (2011) 1981-1989.
- [141] Z. Wang, K. Guan, M. Gao, X. Li, X. Chen, X. Zeng, The microstructure and mechanical properties of deposited-IN718 by selective laser melting, *Journal of Alloys and Compounds* 513 (2012) 518-523.
- [142] D. Deng, *Additively Manufactured Inconel 718: Microstructures and Mechanical Properties*, Linköping University Electronic Press 2018.
- [143] L. Rickenbacher, T. Etter, S. Hövel, K. Wegener, High temperature material properties of IN738LC processed by selective laser melting (SLM) technology, *Rapid Prototyping Journal* (2013).
- [144] F. Abe, K. Osakada, M. Shiomi, K. Uematsu, M. Matsumoto, The manufacturing of hard tools from metallic powders by selective laser melting, *Journal of materials processing technology* 111(1-3) (2001) 210-213.
- [145] K. Amato, S. Gaytan, L. Murr, E. Martinez, P. Shindo, J. Hernandez, S. Collins, F. Medina, Microstructures and mechanical behavior of Inconel 718 fabricated by selective laser melting, *Acta Materialia* 60(5) (2012) 2229-2239.
- [146] Z. Lu, J. Cao, H. Jing, T. Liu, F. Lu, D. Wang, D. Li, Review of main manufacturing processes of complex hollow turbine blades: This paper critically reviews conventional and advanced technologies used for manufacturing hollow turbine blades, *Virtual and Physical Prototyping* 8(2) (2013) 87-95.
- [147] Y. Zhang, Z. Li, P. Nie, Y. Wu, Effect of cooling rate on the microstructure of laser-remelted INCONEL 718 coating, *Metallurgical and Materials Transactions A* 44(12) (2013) 5513-5521.

- [148] X. Wang, X. Gong, K. Chou, Review on powder-bed laser additive manufacturing of Inconel 718 parts, *Proceedings of the Institution of Mechanical Engineers, Part B: Journal of Engineering Manufacture* 231(11) (2017) 1890-1903.
- [149] P. Blackwell, The mechanical and microstructural characteristics of laser-deposited IN718, *Journal of materials processing technology* 170(1-2) (2005) 240-246.
- [150] C. Zhong, A. Gasser, J. Kittel, K. Wissenbach, R. Poprawe, Improvement of material performance of Inconel 718 formed by high deposition-rate laser metal deposition, *Materials & Design* 98 (2016) 128-134.
- [151] T. Trosch, J. Ströbner, R. Völkl, U. Glatzel, Microstructure and mechanical properties of selective laser melted Inconel 718 compared to forging and casting, *Materials letters* 164 (2016) 428-431.
- [152] J. Jiang, X. Xu, J. Stringer, Support structures for additive manufacturing: a review, *Journal of Manufacturing and Materials Processing* 2(4) (2018) 64.
- [153] M.X. Gan, C.H. Wong, Practical support structures for selective laser melting, *Journal of Materials Processing Technology* 238 (2016) 474-484.
- [154] A. Hussein, L. Hao, C. Yan, R. Everson, P. Young, Advanced lattice support structures for metal additive manufacturing, *Journal of Materials Processing Technology* 213(7) (2013) 1019-1026.
- [155] J. Jhabvala, E. Boillat, C. André, R. Glardon, An innovative method to build support structures with a pulsed laser in the selective laser melting process, *The International Journal of Advanced Manufacturing Technology* 59(1-4) (2012) 137-142.
- [156] B. Vandenbroucke, J.P. Kruth, Selective laser melting of biocompatible metals for rapid manufacturing of medical parts, *Rapid Prototyping Journal* (2007).
- [157] S.H. Thakare, Experimental investigation of effect of support structure geometry on the microstructure and metallurgical properties of IN718 parts fabricated by selective laser melting, *Mechanical and Aerospace Engineering*, The University of Texas at Arlington, 2020.
- [158] G.R. Buican, G. Oancea, R.F. Martins, Study on SLM manufacturing of teeth used for dental tools testing, *MATEC Web of Conferences*, EDP Sciences, 2017, p. 03002.

- [159] A.a.R. Ganesh-Ram, Samarth and Ravichander, Bharath Bhushan and Swails, Nahid and Amerinatanzi, Amirhesam, Study on the microstructural and hardness variations of unsupported overhangs fabricated using selective laser melting, 11589 (2021) 1158900.
- [160] I.a.G.i.a. Tolosa, Ferm{\i}n and Zubiri, Fidel and Zapirain, Fidel and Esnaola, Aritz, Study of mechanical properties of AISI 316 stainless steel processed by “selective laser melting”, following different manufacturing strategies, The International Journal of Advanced Manufacturing Technology 51 (2010) 639--647.
- [161] A.a.H. Hussein, Liang and Yan, Chunze and Everson, Richard, Finite element simulation of the temperature and stress fields in single layers built without-support in selective laser melting, Materials & Design (1980-2015) 52 (2013) 638--647.
- [162] M.a.S. Matsumoto, M and Osakada, Kozo and Abe, Fumie, Finite element analysis of single layer forming on metallic powder bed in rapid prototyping by selective laser processing, 42 (2002) 61--67.
- [163] M.a.S. Matsumoto, M and Osakada, Kozo and Abe, Fumie, Finite element analysis of single layer forming on metallic powder bed in rapid prototyping by selective laser processing, International Journal of Machine Tools and Manufacture 42 (2002) 61--67.
- [164] A.T.P.L.S.S.u.f. cutting.
- [165] A.E.-P. Grinder/Polish. <https://iamlab.uta.edu/facilities/>.
- [166] L.L.A.M.H. Tester. http://www.ydjtest.com/a/Micro_Hardness_Tester/114.html.
- [167] R.W. ImageJ, ImageJ, R.W., US Natl Institutes Heal Bethesda, Maryland, USA. 2012. .
- [168] T. Sanviemvongsak, D. Monceau, B. Macquaire, High temperature oxidation of IN 718 manufactured by laser beam melting and electron beam melting: Effect of surface topography, Corrosion Science 141 (2018) 127-145.
- [169] Z.a.L. Dong, Yabo and Wen, Weibin and Ge, Jingran and Liang, Jun, Effect of hatch spacing on melt pool and as-built quality during selective laser melting of stainless steel: Modeling and experimental approaches, Materials 12 (2019) 50.

- [170] B.a.R. Farhang, Bharath Bhushan and Venturi, Federico and Amerinatanzi, Amirhesam and Moghaddam, Narges Shayesteh, Study on variations of microstructure and metallurgical properties in various heat-affected zones of SLM fabricated Nickel--Titanium alloy, *Materials Science and Engineering: A* 774 (2020) 138919.
- [171] Y.a.L. Liu, Z and Jiang, Y and Wang, GW and Yang, Yang and Zhang, LC, Gradient in microstructure and mechanical property of selective laser melted AlSi10Mg, *Journal of Alloys and Compounds* 735 (2018) 1414--1421.
- [172] P. Mignanelli, N. Jones, E. Pickering, O. Messé, C. Rae, M. Hardy, H. Stone, Gamma-gamma prime-gamma double prime dual-superlattice superalloys, *Scripta Materialia* 136 (2017) 136-140.
- [173] W.M.a.L. Tucho, Vidar H and Austb{o}, H{aa}kon and Sjolyst-Kverneland, Atle and Hansen, Vidar, Investigation of effects of process parameters on microstructure and hardness of SLM manufactured SS316L, *Journal of Alloys and Compounds* 740 910--925.
- [174] A.a.N. Takaichi, Takayuki and Joko, Natsuka and Nomura, Naoyuki and Tsutsumi, Yusuke and Migita, Satoshi and Doi, Hisashi and Kurosu, Shingo and Chiba, Akihiko and Wakabayashi, Noriyuki and others, Microstructures and mechanical properties of Co--29Cr--6Mo alloy fabricated by selective laser melting process for dental applications, *Journal of the mechanical behavior of biomedical materials* 21 (2013) 67--76.